Response to Reviewer Comments

Journal: Earth System Dynamics

Title: **Dynamic regimes of the Greenland Ice Sheet emerging from interacting melt-elevation and glacial isostatic adjustment feedbacks**

Authors: Maria Zeitz, Jan Haacker, Jonathan Donges, Torsten Albrecht and Ricarda Winkelmann

MS No: esd-2021-100

MS Type: Research article

First of all, we would like to thank the editor Michel Crucifix and the two reviewers, Kristin Poinar and one anonymous reviewer, for their immensely helpful comments and their efforts to create the detailed reviews! In our revision of the manuscript we addressed the main issues:

1. In order to address the question, if the observed behavior is an artifact, we have now included an additional robustness analysis, including a different initial state and a different solid Earth model. The qualitative behavior remains the same.
2. We have added a more thorough discussion of the Lingle-Clark model
3. We have renamed the dynamic regimes and added a more detailed discussion on the fluctuation times.

We provide detailed answers to all comments below. The reviewers' comments are given in black and the authors' in blue. The changes made to the manuscript can be found at the end of this document (created with latexdiff). In addition to the changes suggested by the reviewers, we have changed the variable name for the mantle viscosity from ν to η, to be more consistent with existing literature, e.g. Bueler et al. (2007), and we have improved Figure 1 visually (without changing its content).

Comment on esd-2021-100

Kristin Poinar (Referee)

Referee comment on "Dynamic regimes of the Greenland Ice Sheet emerging from interacting melt-elevation and glacial isostatic adjustment feedbacks" by Maria Zeitz et al., Earth Syst. Dynam. Discuss., https://doi.org/10.5194/esd-2021-100-RC1, 2022

Summary and general comments:

This manuscript presents a discovery of unforced, long-term fluctuations in the size of the Greenland Ice Sheet. The fluctuations (which are not really oscillations, as they are not strictly regular or repeating) have periods ~80 - 300 kyr and originate from the interactions between the melt-elevation feedback (a positive feedback) and glacial isostatic adjustment (a negative feedback). This has not been previously studied on long (ice age) timescales in the absence of external triggers (e.g., Heinrich events initiated by ocean heat pulses) for a land-terminating ice sheet. The finding of these emergent cycles could be relevant for "deep future" states of the Greenland Ice Sheet, although it is a challenge to imagine a future without climate forcings that would presumably overshadow the internal variability. Regardless, it is an interesting discovery that merits reporting, and this paper is largely successful. I have only minor suggestions, and although they are somewhat numerous, they are all quite attainable.

Many thanks for the review! We understand that imagining a long-term stable climate forcing may seem somehow abstract. Nevertheless we believe that understanding the dynamic response of the GrIS to this comparatively simple forcing lays an important foundation, e.g. for understanding the stability of the Greenland Ice Sheet.

Specific comments:

The authors used a "power spectrum analysis" to identify periods in the ice volume time series. These methods should be explained, if only briefly, and some test for significance should be carried out. The authors state that "The oscillation times do not seem to show a clear dependence on the values for warming, lapse rate or mantle viscosity" (P11 L12). This seems troubling -- wouldn't we expect a clear pattern to emerge within the parameter space? If so, the authors should do additional thinking and put forth possible explanations for the scatter. If not, that is interesting too, and the authors should elaborate on the reasons why this system is not governed regularly.

Many thanks for this comment, which inspired us to look into the oscillation times more closely. As they do not seem to be perfectly regular or symmetric, showing e.g. extended plateaus at high ice volumes with rather brief "dips" in volume (see e.g. gray and pink curve in Figure 2 b), and only a few oscillations fit into the simulation time of 500kyrs, we now chose a slightly simpler approach to analyze the time scales involved. In particular, we identify the average of the minimal and maximal oscillation volume and analyze the times between two intersections of the ice volume curve with that value. Thus we do not only get the oscillation time for a full period (which we have updated), but we can also analyze the half oscillations more carefully. In some cases the time between two "dips" is very long and therefore dominates the oscillation time. We have separated both time scales, the "recovery time" (defined as the average time for the half oscillation going through a minimum, black lines in Figure R1) and the "plateau time" (defined as the average time for a half oscillation going through a maximum, gray lines in Figure R1) .

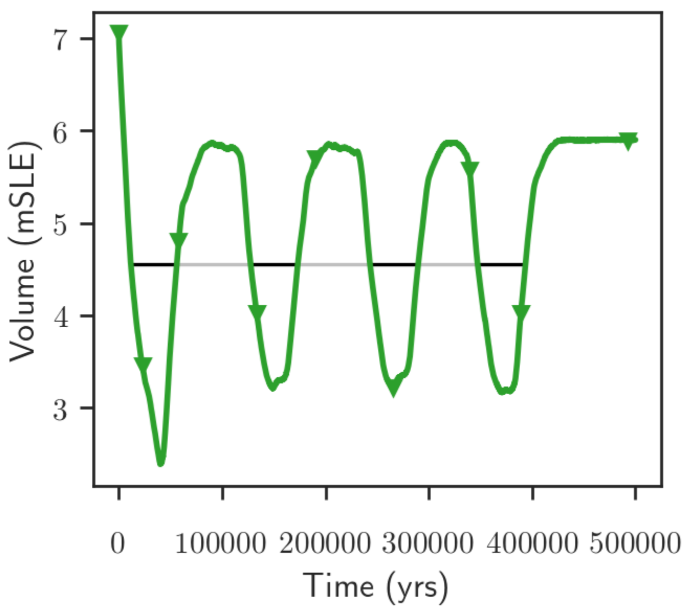

Figure R1: Illustration of recovery time and plateau time. The oscillation of the ice volume is divided into the half oscillation going through the minimum (black lines) and through the half oscillation going through the maximum (gray lines). The volume time series is taken from Figure 2 in the manuscript, with parameters $\Delta T = 2K, \Gamma = 6K/km, \eta = 1 \times 10^{21} Pa\,s$.

We discuss the complex interactions between the recovery time, the depth of the dip, the maximal recovered ice, or the amplitude of oscillation very briefly in the text of the revised manuscript. More importantly, we now analyze the ratio of the recovery time to plateau time. Here a clear pattern emerges: the upper half of the oscillation gets relatively shorter with increasing temperature forcing, increasing mantle viscosity, and most importantly with increasing lapse rate.

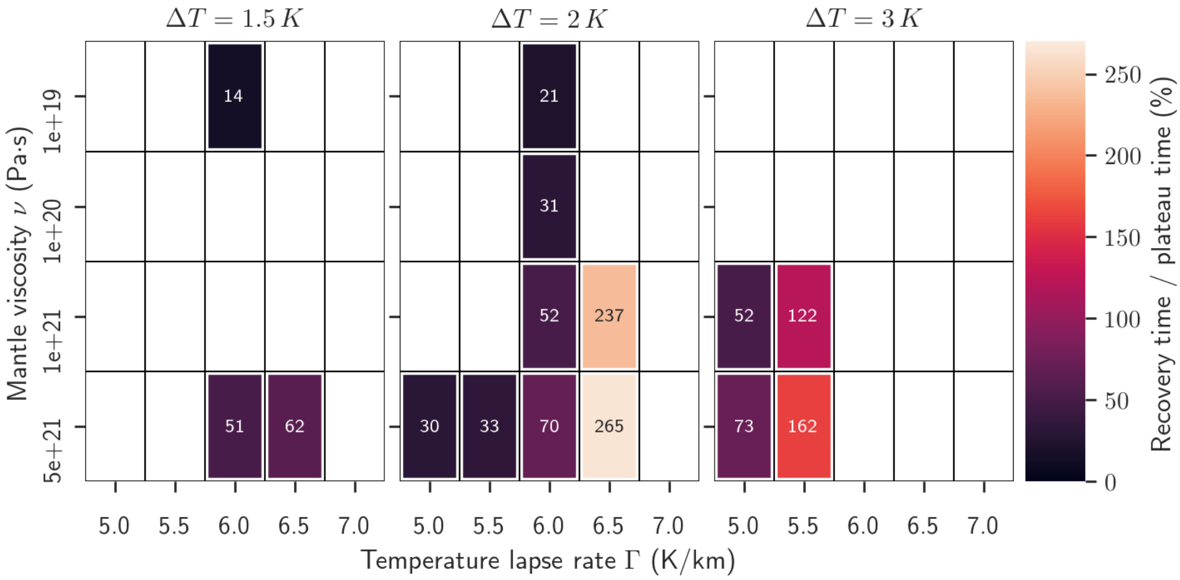

Figure R2: Ratio between recovery time and plateau time for the full factorial parameter space. The numbers in the tiles show the values in %. The larger the ratio, the longer the ice sheet is in a partly recovered state and the shorter the temporary ice losses.

Relatedly, Figure 2 shows that some of the parameter combinations do, apparently, have quite regular periods (especially in Figure 2b), while others do not (such as the higher lapse rates in Figure 2a). A short presentation of the values of the periods (and which are significant) should be done. The significant period values (kyr) could even simply be written inside the cyan blocks of Figure 4.

Thank you very much for the suggestion, we have adjusted the figure accordingly. Concerning the significance: we only identify oscillating states with a minimal amplitude of 0.5m as oscillation dynamics. We have clarified this in the text. In addition we tried using different weights for the average volume depicted in Fig. R1. Shifting it 25% closer to the minimal or maximal volume changed the computed oscillation times by less than 2.5% (less than 1% in most cases), and therefore the uncertainty is less than the variation in period between two oscillations periods.

As alluded to in my summary, I suggest replacing "oscillation" throughout the manuscript with a similar word that does not imply regularity, such as "fluctuation" or even "variation". This is because the sequence of states does not always have a regular repeat interval.

While we understand that the original term suggests a more regular oscillation than we observe, the term “fluctuation” suggests a much more random behavior than we observe. Although the term “variation” might offer some middle ground, we will stick to the original notation, as also suggested by the editor.
In addition the trajectories projected to the bedrock altitude vs. accumulation/ablation plane of the high-dimensional phase space, as shown in Fig. 6 (now Fig. 7 of the revised manuscript), form closed loops in phase space and therefore indicate that regular oscillations appear.
The first six lines of the Discussion restate the results, as do lines 11-17 on this page. These are redundant to the rest of the manuscript and should be removed. The last three lines of the first paragraph describe one possible extended importance of this study, which is not actually studied or discussed, and therefore would be more appropriate in the Conclusion or Introduction.
Thank you for the suggestions, we adapted the manuscript accordingly.
Finally, I would suggest a different name than "recovery" for the state where the ice sheet reaches a new equilibrium size significantly smaller than its start. "Recovery" implies, to me, that the ice sheet returns to its initial state. More precise names could be "re-equilibration" or "new steady state".
Many thanks for bringing our attention to the fact that “recovery” might imply that the Greenland Ice Sheet returns to its initial steady state. We chose this term because it seemed to suggest that the ice volume partly grows back after an initial ice loss. As both suggested terms do not transport this notion, which seems important in the context of the paper, we would rather stick with the term “incomplete recovery”. This should not imply that the full initial ice volume is recovered, but it still tells the story of the regrowth.

Technical corrections:
P1 L5 - "Greenland could become essentially ice-free on the long-term" - I suggest stating the rough number of years found for this, instead of the vague "long-term".
Done
P1 L13 - "oscillation periods of tens to hundreds of thousand of years" - similarly, I suggest stating the rough number of years here. This is because your minimum period (80 kyr) is not that well described by "tens of thousand of years", so it is unintentionally misleading.
Done
P4 L4 - add Laurentide Ice Sheet, which is what Bassis et al. (2017) studied.
Done
P5 L8 - Please include a brief explanation, and/or citation, for why the enhancement factors (1 and 1.5) are different depending on which stress balance is used across the domain.
We included the reference to Ma et al. (2010), as they suggest using different enhancement factors in different flow regimes to reflect the anisotropy of the ice. However, the ratio between the enhancement factors used in our simulations is much less than the suggested ratio of 5-10, it is rather a result of an optimization process, similarly to Aschwanden et al. (2016), which we now also cite in this context, and very much depends on the model resolution.
P5 Sect 2.1 - The level of description of the ice sheet model (2.1.1) is much more general than the earth deformation model (2.1.2). The classic bending-beam PDE (Eq.1) is included with all parameters described and values supplied, for instance, but the sliding law and till stress model used in PISM are only described in words, with no parameter values given. These should be enhanced to match the level of 2.1.2.

Thank you very much for the suggestion. We have improved on the level of detail for the ice sheet modeling part.

P8 L12 - Missing reference (?).

Fixed it

P11 L3 - specify meters global sea level rise; write 1 \times 10^{19} instead of 1e+19

Done

P11 L21 - typo "2astern"

Fixed it

P12 L4 - I have never seen a zero-indexed "0/i/ii/iii" list before. I suggest standardizing to "i/ii/iii/iv".

Done

Table 1 - Specific values used for \Delta T are listed, which is helpful. Values for \Gamma and \nu, instead of their ranges, should be listed similarly.

Done

Figure 2 - Title of panel a is missing the "times" sign. X axis labels in kyr would make it more legible.

Done

Figure 5 - I suggest you outline or stipple the boxes that you classify as oscillating. As it is, the figure relies on the reader to interpret on their own which boxes show "significant difference" in color.

Thank you for the suggestion, we have now highlighted the region where oscillation dynamics take place.

Figure 6 - What is the mantle viscosity & climate change forcing (\Delta T) used here? It looks like it might be the same runs shown on Figure 2a, but that is only my guess.

Done

Anonymous Referee #2

Referee comment on "Dynamic regimes of the Greenland Ice Sheet emerging from interacting melt-elevation and glacial isostatic adjustment feedbacks" by Maria Zeitz et al., Earth Syst. Dynam. Discuss., https://doi.org/10.5194/esd-2021-100-RC2, 2022

General comments

The paper documents intriguing dynamic behaviour of the Greenland ice sheet resulting from the interplay between the melt-elevation feedback and the GIA feedback. The material is generally well presented and easy to follow. By itself the results are very interesting and potentially provide a very novel insight into the longer-term internal dynamics of the coupled climate-ice sheet-bedrock system. At the same time, I am also very puzzled by the results, in particular by the self-sustained quasi-periodic oscillations the authors find for (a rather narrow range) of parameter combinations. Many Greenland ice sheet modelers have performed similar experiments already since the early 1990s by imposing a stepwise warming in very similar model setups involving quasi the same degree-day type of climate forcing and taking into account isostasy with state-of-the-art models, but none of these studies have ever found even a trace of the kind of oscillations described in the paper. This makes me conclude that indeed their oscillatory behaviour may well be an 'artifact' (to cite their own words) of their particular experimental design and parameter choice. In other words, their model behaviour is probably not a very robust type of behaviour, to say the least, and might be very difficult to replicate in other models. My suspicion is that their model behaviour is a result from the particular choice of the Lingle-Clarke isostatic model and will not show up for any other isostatic model, be it of the 'ELRA' type, or of the more sophisticated 'self-gravitating visco-elastic earth model' type.

I think the paper would be a very valuable addition to the literature of Greenland ice sheet dynamics, but first I would like to find out more on the robustness of the results and the specific role played by isostasy. A particular feature of the Lingle-Clarke model, and its implementation by Bueler et al. (2007) is that the relaxation time increases for wavelengths up to a few thousand km (a wavelength corresponding to the Greenland situation), which I believe is unrealistic. Full visco-elastic models show the contrary, the relaxation time decreases for a larger load. My guess is that it is exactly this specific behaviour of the LC model that is causing the oscillations. I suggest the authors make an effort to respond to this criticism by including material (figures and/or discussion) to prove or disprove this point.

Thank you very much for this comment. As the oscillation dynamics can be interpreted as a result of two competing feedbacks, as described in Fig. 1 and Fig. 4 of the manuscript, which manifests over a wide range of parameters and modeling choices (see discussion below), we do not think that it is an 'artifact' of this particular modeling setup alone. Talking to other ice-sheet modelers revealed that experiments with a constant climate forcing on time scales of many hundreds of millenia are performed less often compared to e.g. paleo climate forcing or sea-level rise experiments on shorter time scales. Therefore it may be less surprising that this dynamic regime has not been reported in the literature yet.

In order to test if the oscillatory behavior is an artifact of the bedrock model alone, we tested some experiments with the already implemented point-wise isostasy model, an instantaneous pointwise adaption of the bedrock to changes in load

$$b(t, x, y) = b(0, x, y) - \frac{\rho_i}{\rho_m}[H(t, x, y) - H(0, x, y)].$$

Here $b(t, x, y)$ is the elevation of the bedrock at a given time and location, $H(t, x, y)$ is the ice thickness at a given time and location and ρ_i and ρ_m are the density of the ice and the mantle, respectively. Simulations with this most simple bedrock model do show very similar oscillations, even though the amplitude and the oscillation time differ from the oscillation which appear with the Lingle-Clark model, see Fig. R3 a. We show and discuss these results in a new subsection dealing with robustness towards several modeling choices.

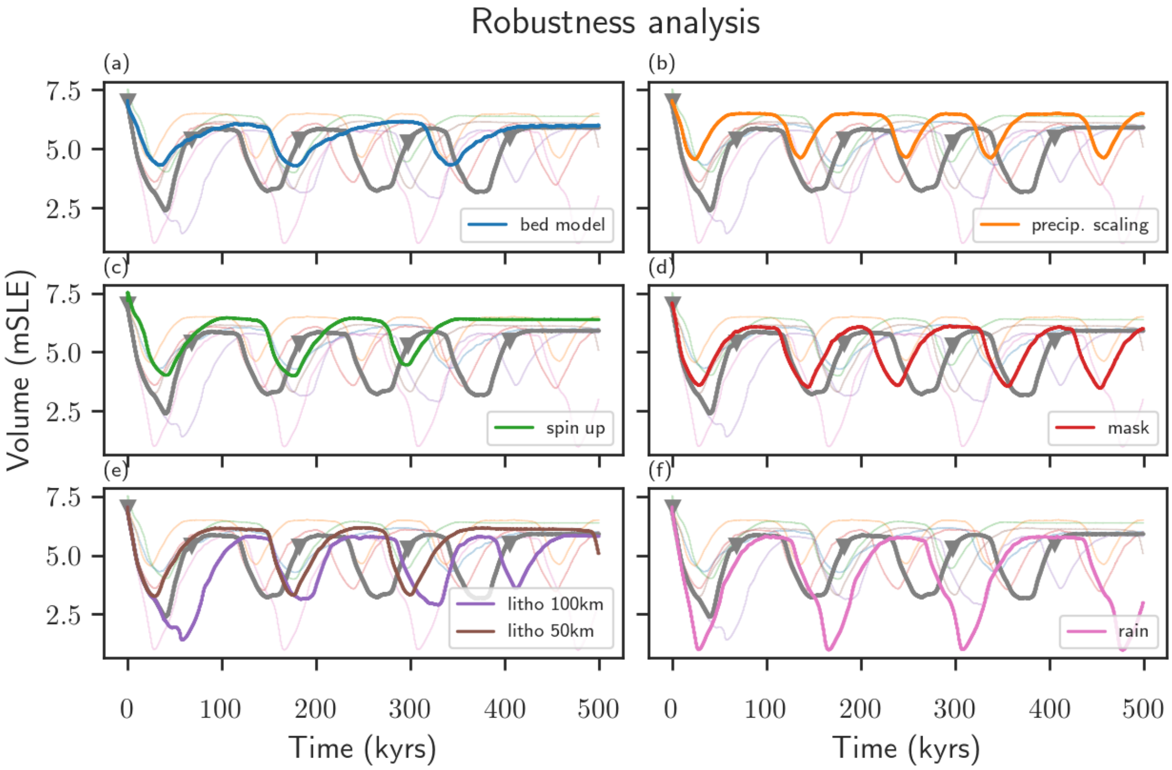

Figure R3: Robustness analysis for the simulation run with parameters $\Delta T = 2\mathrm{K}$, $\Gamma = 6\mathrm{K/km}$, $\eta = 1 \times 10^{21}\mathrm{Pa\ s}$. *The gray curve shown in each panel corresponds to the reference run as described in the paper. Robustness tests are shown in color with faint, thin lines. One curve is highlighted in each panel to increase readability. (a) comparison to the pointwise isostacy model, described in the equation above. (b) comparison to a run, which includes a precipitation increase of 7.3% for every one degree Celsius of global mean temperature increase. (c) comparison of different spin-ups. The green curve has been spun up with two glacial cycles, while the gray curve was spun with a constant climate. (d) comparison to a run without flux correction. (e) comparison with different lithosphere thicknesses. The lithosphere flexural rigidity was varied corresponding to two different effective lithosphere thicknesses of 50km and 100km. The reference run assumes a lithosphere thickness of 88km. (f) comparison with a different interpolation for the transition between rain and snow.*

Moreover, a discussion with Michele Petrini revealed that he indeed observes long-term oscillations with a constant climate forcing using the ELRA bedrock model and a lapse rate of 6K/km. The peer-reviewed publication showing these results is forthcoming; a first glimpse can be found in the display materials of the 2021 EGU contribution.

In addition to the changes in amplitude and oscillation time, which can be seen above, a shift in the dynamic landscape (Fig. 4) might be a consequence of alternative modeling choices. For example when combining the glacial spin-up with the no flux correction (see panels c and d), the response of the Greenland Ice Sheet changes from “oscillation” to “partial recovery”. Performing new simulations for the full factorial parameter space for each possible combination of modeling choices is sadly beyond the scope of this paper.

Having performed a suite of robustness experiments with different modeling choices, we still find the qualitatively similar oscillating behavior. We therefore conclude that the oscillating regime is fairly robust and not an artifact driven by the choice of the solid Earth model alone.

Specific comments

page 2, line 5: a reference is needed to substantiate the 65/35% attribution of current ice losses of the Greenland ice sheet. As far as I am aware from comprehensive studies, the ratio is more like 50/50 for both SMB changes and ice calving changes (e.g . IMBIE team, 2020)

Thank you for the comment. We have added the IMBIE reference and adjusted the numbers. The original numbers were taken from Mouginot et al. (2019) and it is an average value over the period from 1972 - 2018. However, with increasing warming the changes in climatic mass balance have become more important (Mouginot et al. (2019) find 55% for the period 2000-2018).

page 2, line 22: here, and elsewhere (page 6, line 5) it is stated that 'to our knowledge' their have been no previous studies coupling Greenland ice-sheet dynamics to bedrock dynamics. That is not entirely true. Le Meur and Huybrechts (1998, also in GJI in 2001) have done this for the glacial cycles, also in Zweck and Huybrechts (2005) Greenland ice sheet dynamics was included and was part of the sensitivity study.

Thank you very much for bringing our attention to this. We have included these references to the manuscript and have clarified the sentence to "However, the interaction of the negative bedrock uplift feedback and the melt-elevation feedback, has, to our knowledge, not yet been systematically studied in the context of the Greenland Ice Sheet".

page 4, line 11: explain what the 'small ice cap instability' is.

Done

page 4, line 12: To what does 'This' refer?

We have clarified this sentence.

page 4, line 17: explain why the factor 1/3 is expected.

The ⅓ stems from the difference in densities. As the asthenosphere is approximately three times more dense than the ice, Archimedes' principle allows us to estimate the amount of uplift after a change in ice load. We have included this in the manuscript.

page 6, section 2.1.2: a critical appraisal of the specific features of the LC model is in order here. A more thorough discussion of the dependence of the relaxation time on the wavelength of the load change and how this compares to other models is required here, as this may well be a crucial issue in this paper.

The widely used ELRA model assumes one single relaxation time for the solid Earth response, independent of the wavelength of the load change, the Lingle Clark model in contrast includes the viscosity of the mantle explicitly, and therefore the relaxation time depends on the wavelength of the load change. Some discussion is already performed in Bueler et al. (2007), but we now show how the relaxation time vs. wavelength of the load change depends on mantle viscosity in the appendix of the revised manuscript.

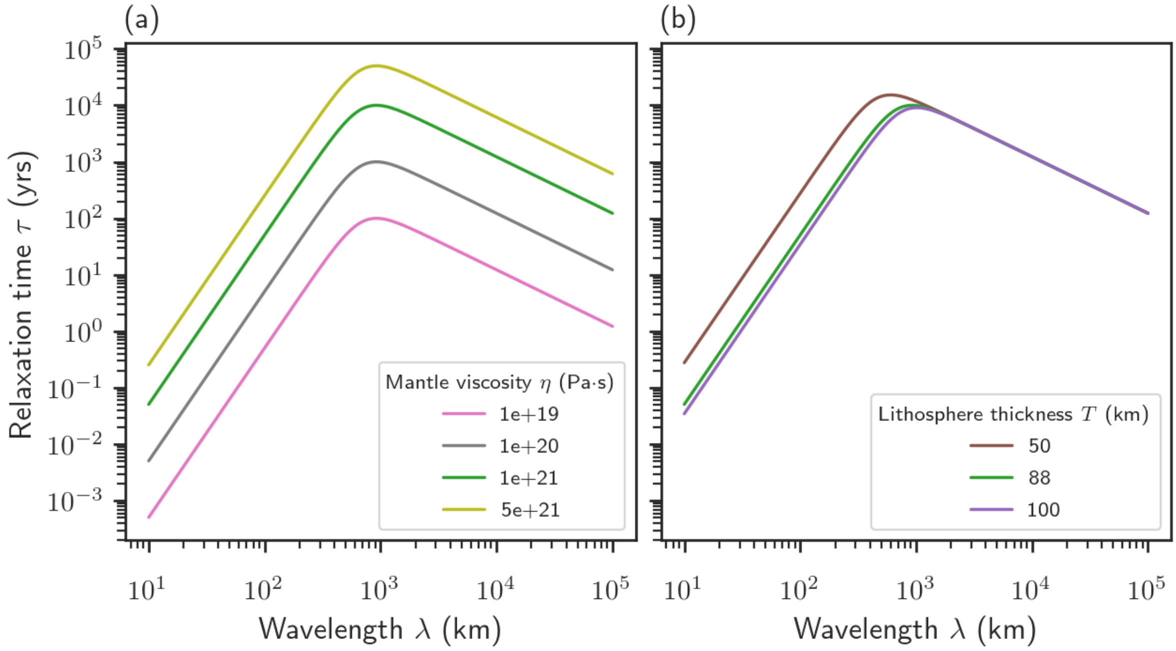

Figure R4: Relaxation times of the Lingle-Clark model vs. wavelength of the load change. Relaxation times are computed as in Bueler et al. (2007), Eq. (14).

In contrast to more complex solid Earth models, the Lingle-Clark model exhibits only one single mode of the spectrum, the mantle mode M0. For a two layer model with a compressible elastic lithosphere over an viscous half-space with $\eta = 1 \times 10^{21}$ Pa s, the M0 mode has a maximal relaxation time of 10,000 years for a wavelength of approx. 300 km (see Klemann, 2003), the LC model represents this behavior well. Solid Earth models which include more layers exhibit also more modes of the spectrum. The additional modes in e.g. a four-layer model show a monotonous strong increase of relaxation time with increasing wavelength and decreasing wavenumber (Klemann 2003).

We now include a more detailed discussion of these features in the revised manuscript. However, we do have reason to believe, that the oscillations are not a feature of the LC model in particular, as they also arise when using the pointwise isostatic model (as shown in the robustness analysis), which has an instantaneous response time independent of the wavelength, as well as for the ELRA model as studied bei Petrini et al..

page 6, section 2.1.3: apparently the precipitation pattern from RACMO does not interact with climate change or ice sheet geometry as it seems to be fixed. Mention this explicitly and mention the shortcomings of such an approach.

We now mention the fact that the precipitation does not scale with temperature more explicitly and we briefly discuss that this makes the experiments less realistic. However, this idealized approach brings us a bit closer to the as well idealized feedback loop in Figure 1. We now also show in the robustness analysis that the simulations, which increase the precipitation by 7% per degree of warming show the same qualitative behavior in the oscillating regime, however, the amplitude of the oscillation is dampened by the increase in accumulation.

page 7, section 2.1.3: is the rain fraction a function of the monthly mean temperature? If so, the transition temperature range between 0 and 2°C seems much too small. One would still expect rainfall during a month with a mean temperature below 0°C and snowfall for a mean temperature above 2°C. Please discuss the limitations of this approach.

PISM is a stand-alone ice sheet model, which relies on input for atmospheric variables like precipitation or near surface air temperature. The interpolation described here is the standard for how PISM treats precipitation and it allows change between snow and rain depending on the temperature. A linear transition between rain and snowfall is a very simple approximation of more complex processes which would of course be best described with a fully coupled atmospheric model. We now include an additional run, which has a broader transition range, from -1°C to +3°C, which also shows oscillating behavior, but with a higher amplitude (see Fig. R3 f).

page 7, line 16: it is mentioned that ice-ocean interaction is included via PICO. More information is needed here. Where is the ocean forcing coming from? At what resolution? What about water circulation in the fjords? How is oceanic forcing transferred to calving fronts? Does the model have a grounding line and attached ice shelves, and how are they treated? Does it matter to include ocean forcing for the type of experiments described here at all?

We generate the ocean forcing ourselves by using a scalar anomaly on the World Ocean Atlas data. The ocean warming corresponds to 70% of the global mean temperature anomaly. The WOA data is remapped onto the PISM simulation grid. The data is averaged over the extended drainage basins of the GrIS. Here the average value is applied for each extended drainage basin, even if the ice sheet retracts. PICO calculates the sub-shelf melt rate; it is not suited to compute the plume-driven frontal melt of a tidewater glacier without a floating tongue. The calving process is computed through von Mises calving and a minimal floating thickness of 50m.

It is true that the ocean forcing might not be necessary for this kind of experiment, as the floating ice tongues make up less than 0.2% of the ice sheet area.

page 7, section 2.2.1, and associated figures in the supplement: it is puzzling to me that while the climatic mass balance from the model differs substantially from RACMO (Fig. S2), the simulated ice sheet domain almost exactly matches the observations (Figs. S1 and S3). Almost on view it can be seen that the ice-sheet wide average surface mass balance must be positive over the domains shown, yet there is hardly any advance of the margin for the initial state. How was the initial ice sheet constrained? What is the meaning of the row of black points (low or zero velocity) at the margin in Fig. S3? To me it is hard to believe that the initial state corresponds to a self-sustained steady-state ice sheet with a freely evolving margin, the latter of which is crucial in the experiments.

Yes, it is correct that we used a flux correction for the zones, which are ice-free under the present day climate. Ice sheet models forced with the precipitation fields from RCMs often overestimate the accumulation in the South East and therefore an ice sheet in present-day climate would grow in volume. As we perform warming experiments, where the ice sheet experiences retreat, we do not think that including such a flux correction should affect the results on long time scales. We now provide a simulation run, which does not use the flux correction on the ice-free margin and we still observe oscillations, which is found in the robustness analysis section.

A consequence of removing the mask is that the control run stabilizes at slightly higher ice volumes (from 7.06m to 7.62m).

We have included a better discussion of this in the paper.

page 12 and further, section 3.2: A crucial issue is how realistic the bedrock model is. In the model only viscosities are changed to control the relaxation time scale. What about the effect of variations in flexural rigidity of the lithosphere?

We have performed runs with two additional elastic lithosphere thicknesses, which all show qualitatively similar behavior. It is noticeable though, that thicker lithospheres show a stronger initial ice loss than thinner lithospheres. Both additional simulations are similar in amplitude and oscillation time. Note that the LC model does not include lithosphere thickness directly but through the flexural rigidity.

page 14, figure 6: The figure is very difficult to read and understand, and should be improved. The colour saturation seems to represent time (but the caption does not say), however the pale parts of the lines are difficult to see. What is the meaning of both crosses? Lower axis: accumumlation-> accumulation. Left axis: are you sure the average level of topography has negative values? Please adapt the figure and the caption to increase readability.

Thank you very much for the comment. We noticed an error in the python script used for the analysis and now fixed the mistake which led to negative average bedrock topography values. In addition we have improved the visual readability of the figure, by adjusting the color scale and adding the initial states (which is the meaning of the crosses) to the legend. The caption is now also improved.

In our opinion the figure, even if a bit unusual in the ice-sheet modeling context, provides a nice visual representation of the oscillatory behavior. The trajectory of the oscillation dynamics forms closed loops in phase space (or rather when projected to this plane of the high-dimensional phase space), similar to a non-linear oscillator or a limit-cycle.

We have shortened the discussion of the figure and removed the last sentence of the paragraph, as the correct trajectories now intersect.

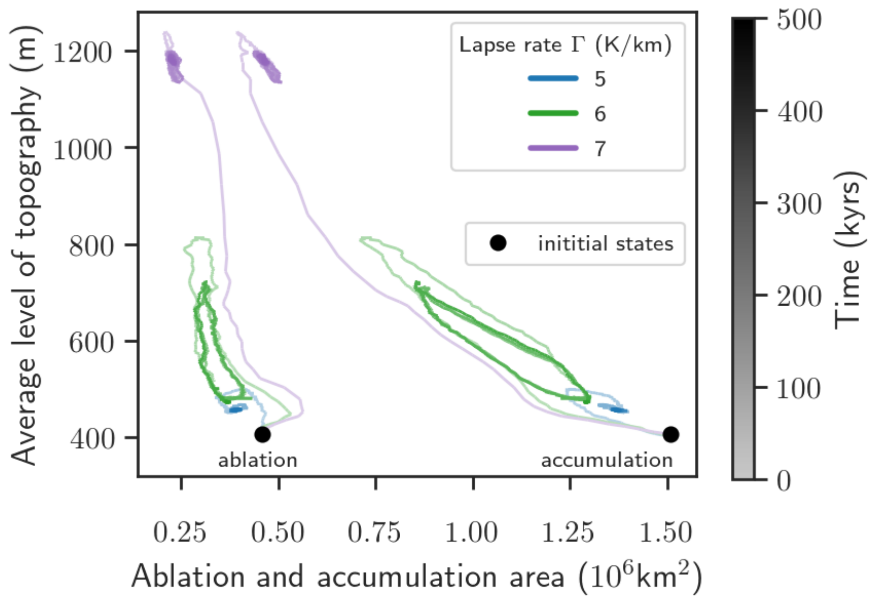

Figure R4: Corrected trajectories projected onto one plane of the phase space. Compare with Fig. 6 in manuscript.

Page 15, lines 18-20: it is impossible to discern on Figure 6 the clockwise or counterclockwise sense of the trajectories. Perhaps an arrow would help.

Thank you for the suggestion, we have included arrows in the revised manuscript.

Page 16, line 31: Petrini et al. (2021) is a crucial reference to prove that the results are not an artifact of the specific experimental design. However, that is an EGU abstract, and cannot be checked. Remove the reference to Petrini et al. (2021).

The robustness tests we have included now should provide sufficient evidence that the observed behavior is most likely not an artifact, and almost certainly not an artifact of the LC model.
Petrini et al. observed oscillations in long-term warming runs with the CISM ice sheet model coupled to an ELRA model, when forced with a constant climate from CESM SMB. Those oscillations are regular with an approximate period of 30-40kyears. While the abstract alone is not a good enough reference, the interested reader will find the "display materials" showing the time series of the above-mentioned runs, linked to the abstract
(https://presentations.copernicus.org/EGU21/EGU21-12958_presentation.pdf). Instead of citing the EGU contribution we could cite the display materials directly as a web page, if this is more suitable. This should provide a first impression to the reader, while the peer reviewed scientific publication is being prepared by Petrini and his co-authors.

Technical corrections

Page 3, line 14: solte -> solve
Page 3, line 32: sophisticates -> sophisticated
Page 3, line 33: year of Fettweis et al. publication missing
Page 4, line16: add 'itself' between 'manifest' and 'on'
Page 8, table 1: the mantle viscosity value of 1x1**-19 cannot be right.
Page 8, line 12: there is a '?' in the reference list
Page 8, line 22: remove the comma between 'both' and 'the'.
Page 14: line 11: do not start a sentence with a capital after a semi-colon
Page 16, line 31: Hoever -> However
We have corrected the manuscript accordingly.

Comment on esd-2021-100

Michel Crucifix (Editor)

Dear authors,

After a (somewhat) long wait, the two reviews are in. What you show in your paper can, in my view, be called 'oscilations' (even if not perfectly periodic), and oscillations in glacial/isostatic systems are rare, though not quite unprecedented (Oerlemans, J. Glacial cycles and ice-sheet modelling. Climate Change, **4,** 353–374 (1982). https://doi.org/10.1007/BF02423468. The context was quite different, as well at the overall setup, but this old example suggests, as pointed out by reviewer 2, that assumptions invoved in the lithosphere/asthenosphere model are crucial. I would therefore invite you to consider the possibility of sensitivity experiments that would adress the question, though I would not be willing to substantially delay the publication of your study.

Many thanks for bringing our attention to the publication by Oerlemans, discussing free oscillations in a conceptual model including an ice sheet, a simplified melt-elevation feedback and a simple bedrock uplift model with one single relaxation time. In fact we believe that this paper strengthens our point, as it shows that unforced oscillations can emerge from the feedbacks involved in a variety of modeling assumptions, given that the system is “nonlinear enough” and includes thermodynamics. There the occurrence of oscillations depends on snow-line slope, the maximal accumulation rate and the representation of thermodynamics. The bedrock parameters were not part of the study. We now include a reference to this publication in the discussion.

Dynamic regimes of the Greenland Ice Sheet emerging from interacting melt-elevation and glacial isostatic adjustment feedbacks

Maria Zeitz[1,2], Jan M. Haacker[1,2,3], Jonathan F. Donges[1,4], Torsten Albrecht[1], and Ricarda Winkelmann[1,2]

[1]Earth System Analysis, Potsdam Institute for Climate Impact Research, Member of the Leibniz Association, Telegrafenberg A31, 14473 Potsdam, Germany

[2]Institute for Physics and Astronomy, University of Potsdam, Potsdam, Germany

[3]Delft University of Technology, Faculty of Civil Engineering and Geosciences, Department of Geoscience and Remote Sensing, Delft, The Netherlands

[4]Stockholm Resilience Centre, Stockholm University, Kräftriket 2B, 11419 Stockholm, Sweden

Correspondence: Maria Zeitz (maria.zeitz@pik-potsdam.de), Ricarda Winkelmann (ricarda.winkelmann@pik-potsdam.de)

Abstract. The stability of the Greenland Ice Sheet under global warming is governed by a number of dynamic processes and interacting feedback mechanisms in the ice sheet, atmosphere and solid Earth. Here we study the long-term effects due to the interplay of the competing melt-elevation and glacial isostatic adjustment (GIA) feedbacks for different temperature step forcing experiments with a coupled ice-sheet and solid-Earth model. Our model results show that for warming levels above 2°C, Greenland could become essentially ice-free ~~on the long-term~~within several millenia, mainly as a result of surface melting and acceleration of ice flow. These ice losses ~~can be~~ are mitigated, however, in some cases with strong GIA feedback even promoting ~~the partial~~ an incomplete recovery of the Greenland ice volume. We further explore the full-factorial parameter space determining the relative strengths of the two feedbacks: Our findings suggest distinct dynamic regimes of the Greenland Ice Sheets on the route to destabilization under global warming – from incomplete recovery, via quasi-periodic oscillations in ice volume to ice-sheet collapse. In the incomplete recovery regime, the initial ice loss due to warming is essentially reversed within 50,000 years and the ice volume stabilizes at 61-93% of the present-day volume. For certain combinations of temperature increase, atmospheric lapse rate and mantle viscosity, the interaction of the GIA feedback and the melt-elevation feedback leads to self-sustained, long-term oscillations in ice-sheet volume with oscillation periods ~~of tens to hundreds of thousands of~~ between 74 and over 300 thousand years and oscillation amplitudes between 15-70% of present-day ice volume. This oscillatory regime reveals a possible mode of internal climatic variability in the Earth system on time scales on the order of 100,000 years that may be excited by or synchronized with orbital forcing or interact with glacial cycles and other slow modes of variability. Our findings are not meant as scenario-based near-term projections of ice losses but rather providing insight into of the feedback loops governing the "deep future" and, thus, long-term resilience of the Greenland Ice Sheet.

1 Introduction

The Greenland Ice Sheet (GrIS) holds enough water to raise global sea levels by more than 7.4 m and is continuously losing mass at present, thereby contributing to global sea-level rise (Morlighem et al., 2017; Frederikse et al., 2020). Current mass loss rates of 286 Gt/yr are observed, a 6-fold increase since the 1980's (Mouginot et al., 2019). ~~Here,~~ While historically approximately 35 % can be attributed to a decrease in climatic mass balance and 65 % ~~are due~~ to an increase in ice discharge (Mouginot et al., 2019), the ratio has already shifted to approximately 50/50 (Mouginot et al., 2019; IMBIE Team, 2020). While it has been suggested that the Greenland Ice Sheet could become unstable beyond temperature anomalies of $1.6-3.2\,^{\circ}\mathrm{C}$ due to the self-amplifying melt-elevation feedback (Levermann and Winkelmann, 2016), recent studies debate whether a tipping point might have already been crossed (Robinson et al., 2012; Winkelmann et al., 2011; Boers and Rypdal, 2021). Understanding the feedback mechanisms and involved time scales at play in GrIS mass loss dynamics is necessary to understanding its stability under climatic changes.

Changing climatic conditions during the glacial cycles had a strong influence on the ice volume of the Greenland Ice Sheet. It varied from 3-7 m sea-level equivalent (that is the volume above floatation, divided by the total ocean area) in the last interglacial (from 126 to 115 kyrs BP) to 12 m during the last glacial maximum (19-20 kyrs BP) (Vasskog et al., 2015), while the present day volume of the GrIS is 7.42 m. Various processes and feedbacks in the ice sheet, atmosphere, ocean and solid Earth governing the ice dynamics, like ice-ocean interactions, the melt-elevation feedback, and the snow-albedo feedback played an important role in past transitions from interglacial to glacial and vice versa (Denton et al., 2010; Willeit and Ganopolski, 2018; Pico et al., 2018). In this way, the GrIS has been a key component in the emergence of glacial cycles and their implications for overall Earth system stability, as can also be analyzed from a dynamical systems point of view (Crucifix, 2012). Simple models also allow to study the "deep future", i.e. the future on time scales beyond the ethical time horizon as defined e.g. by Lenton et al. (2019), of the Greenland Ice Sheet and the Earth system and reveal that anthropogenic CO_2 emissions affect the climate evolution for up to 500 kyrs and can postpone the next glaciation (Talento and Ganopolski, 2021).

~~One particular feedback~~ The influence of the bedrock uplift onto the dynamics of the Greenland Ice Sheet has been studied with self- gravitating spherical viscoelastic solid Earth models in glacial cycle simulations by e.g. Le Meur and Huybrechts (1998, 2001) . A study systematically varying the isostacy parameters was performed by Zweck and Huybrechts (2005) for the last glacial cycle. However, the interaction of the negative bedrock uplift feedback and the melt-elevation feedback, has, ~~which,~~ to our knowledge, ~~has~~ not yet been explicitly and systematically studied in the context of the Greenland Ice Sheet ~~, is the negative feedback in the interaction between the ice sheet and solid Earth~~ (Pico et al., 2018). Here we aim to close this research gap, by systematically exploring how the feedback between solid Earth, ice, and climatic mass balance and their interactions affect the long term response of the Greenland Ice Sheet.

Changes in ice load lead to glacial isostatic adjustment (GIA), a decrease in ice load initiates an uplift with characteristic time scales of hundreds to thousand of years (Barletta et al., 2018; Whitehouse et al., 2019). Currently observed post-glacial uplift rates in Greenland range between -5.6 mm/yr and 18 mm/yr (Adhikari et al., 2021; Wahr et al., 2001; Dietrich et al., 2005; Schumacher et al., 2018; Khan et al., 2008). Some studies suggest that uplift rates are higher in the South East, where the Iceland hot spot has possibly passed, which can be associated with locally low viscosities in the upper mantle (Khan et al., 2016).

The viscous bedrock response is generally assumed to be slow compared to ice losses, with characteristic response time scales of tens to hundreds of millennia. However, several studies suggest that the viscosity of the asthenosphere and the upper mantle varies spatially and could be locally lower than previously thought (e.g. in Iceland, Patagonia, the Antarctic peninsula, Alaska). This implies that the time scale of the viscous response to changes in ice load might be much shorter, e.g. close to tens or hundreds of years (Whitehouse et al., 2019). The elastic response component responds on an even faster time scale to changes in ice load, e.g. the 2012 extreme melt event caused a significant peak in GPS measured uplift rates (Adhikari et al., 2017). A model of the solid Earth can help to interpret the GPS measurements in order to distinguish the elastic uplift caused by recent mass losses from the delayed viscous uplift caused by the retreat of ice since the last glacial maximum, and deduce solid earth parameters like mantle viscosity and lithospere thickness (Adhikari et al., 2021; Schumacher et al., 2018).

Efforts to model the solid earth response to changes in ice load range from local one-dimensional representations of the bedrock uplift to full three-dimensional models. The ELRA-type of model represents the solid earth as an Elastic Lithosphere and a Relaxing Asthenosphere ~~by assigning~~ and assigs a single time constant to the ~~uplift~~ relaxation response (Le Meur and Huybrechts, 1996; Zweck and Huybrechts, 2005). These models are computationally efficient and are often coupled to ice-sheet models in long-term simulations (Robinson et al., 2012). The Lingle-Clark model expands the elastic plate lithosphere with a viscous half-space and solves the equations explicitly in time (Lingle and Clark, 1985; Bueler et al., 2007). The relaxation time of the solid earth then depends on the spatial wavelength of the perturbation in ice load~~.~~, as shown in Fig. A1. However, this model uses only one constant value for the mantle viscosity, it does not include vertical or horizontal variations, nor does it ~~solte~~ solve the sea-level equation including self-consistent water-load changes or the rotational state of the Earth (Farrell and Clark, 1976; Hagedoorn et al., 2007) Such a model can be expanded to include more layers, e.g. the lower mantle, and take additional model of the relaxation time spectrum into account; however, it becomes more difficult to constrain (Lau et al., 2016). One-dimensional solid earth models explicitly consider the spherical shape of the Earth instead of assuming a half space (Tosi et al., 2005; Fleming and Lambeck, 2004; Simpson et al., 2009; Lambeck et al., 2014)~~. However,~~ , but they do not represent lateral variations ~~in~~ of solid-Earth parameters. Three dimensional models, which resolve not only several layers of the vertical dimension, but include additional variability in the horizontal direction, ~~are developed to~~ account for the ongoing discovery of lateral variations in mantle viscosity and lithosphere thickness (Khan et al., 2016; Whitehouse, 2018; Whitehouse et al., 2006, 2019; Haeger et al., 2019; Martinec, 2000). A laterally varying 3D model can change the estimate of projected global mean sea-level rise due to an ice-sheet collapse in the West-Antarctic by up to 10% compared to a 1D model (Powell et al., 2021). Inferred values for mantle viscosities can span several orders of magnitude and therefore substantially impact the estimate of bedrock uplift rates as a response to present day ice losses (Powell et al., 2020). So far the coupling efforts between 3D solid-Earth models and physical ice-sheet models have been focused mostly on the Antarctic Ice Sheet, exploring the feedback between solid Earth and ice sheets and its potential to dampen or inhibit unstable ice sheet retreat (Gomez et al., 2013; De Boer et al., 2014; Gomez et al., 2018, 2020). Self-gravitation effects affect the stability of the grounding line (Whitehouse et al., 2019; Pollard et al., 2017) and GIA models which self-consitently solve the sea-level equation are crucial. Ongoing work focuses on the northern hemisphere, coupling for instance the Parallel Ice Sheet Model PISM to the solid-Earth model VILMA.

Similarly, modeling efforts of the climatic mass balance of the Greenland Ice Sheet range from computationally efficient temperature index models over energy balance models to ~~sophisticates~~ sophisticated regional climate models, an overview can be found in the model intercomparison effort by ~~Fettweis et al.~~ Fettweis et al. (2020).

The response of the solid earth to ice loss can be part of a negative, meaning counteracting or dampening, feedback loop, called glacial isostatic adjustment (GIA) feedback, that can mitigate further ice loss. Studies focused on the GIA feedback in context of the Antarctic Ice Sheet and the Laurentide Ice Sheet suggest that the bedrock uplift can lead to a grounding line advance and therefore has a stabilizing effect on glaciers that are subjected to the marine ice sheet instability (MISI) (Whitehouse et al., 2019; Konrad et al., 2015; Kingslake et al., 2018; Bassis et al., 2017; Barletta et al., 2018). However, to our knowledge the GIA feedback has not yet been addressed in the context of the Greenland Ice Sheet, where, in comparison to the Antarctic Ice Sheet, marine terminating glaciers contribute less to mass loss.

The feedback cycle we explore in this study is ~~rather~~ related to the self-amplifying melt-elevation feedback. The melt-elevation feedback establishes a connection between ice thickness and climatic mass balance: the lower the surface elevations the higher are typically temperatures and associated melt rates (see also Figure 1, in particular the ~~orange~~ red arrows). An initial increase in melt thins the ice, bringing the ice surface to lower elevation. Subsequently the temperature increases and amplifies both, melt rates and ice velocities, and therefore leads to further ice loss and thinning. Once a critical thickness is reached this feedback can lead to a destabilization of the ice sheet and irreversible ice loss (Levermann et al., 2013). (A similar feedback has also been known as the small ice cap instability~~(Weertman, 1961)~~, assuming constant accumulation rates above an elevation h_S and constant ablation rates below this elevation. Under these conditions a small ice cap can become unstable and expand or similarly a large ice sheet can become unstable and collapse to nothing upon small changes in the parameters (Weertman, 1961).).

~~This formulation of the~~ The instability of the of the melt-elevation feedback, as studied by Levermann and Winkelmann (2016) , assumes a static bed, so that changes in ice thickness equal changes in ice surface altitude. GIA can mitigate this feedback: Due to bedrock deformation changes in ice thickness do not directly translate to changes in surface elevation. The loss of ice reduces the load on the bedrock and allows for a bedrock uplift, damperning the melt-elevation feedback (see blue arrows in Figure 1). Due to the high viscosity of the mantle the glacial isostatic adjustment can manifest on a slower time scale than the climatic changes which cause the ice losses in the first place.

From a static point of view a compensation of approximately 1/3 of ice thickness thinning due to GIA would be expected from Archimedes' principle, given that the ice density ($\rho_i = 910\,\mathrm{kg/m^3}$) is approximately 1/3 of the asthenosphere density ($\rho_r = 3300\,\mathrm{kg/m^3}$). In this study, we explore how the dynamic interaction of the feedbacks allows the GIA feedback not only to dampen but to (periodically) overcompensate for the melt-elevation feedback. Here we focus on the long-term stability of the Greenland Ice Sheet and how it is affected by the positive melt-elevation feedback on the one hand and the negative GIA feedback on the other hand. We use simple representations of both, the melt-elevation and the GIA feedbacks, to study the interplay between them: The melt-elevation feedback is represented by an atmospheric temperature lapse rate which affects the

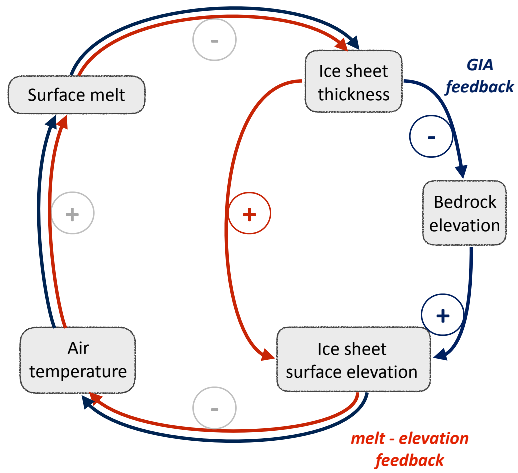

Figure 1. Interacting feedback loops for the proposed glacial isostatic adjustment feedback (GIA feedback). The ~~orange~~ red part indicates the melt-elevation feedback: Higher air temperatures lead to decreasing climatic mass balance. This in turn leads to a decreasing ice thickness and in consequence to a decreasing ice surface elevation. If the surface elevation decreases, the air temperature rises due to the atmospheric lapse rate. This further decreases the climatic mass balance and leads to a positive (enhancing) feedback cycle. The timescale of this feedback cycle is driven by changes in the climate and is typically comparably fast. The blue part shows the counteracting mechanism of the ice load-bedrock uplift feedback. The decreasing ice thickness reduces the load on the bedrock, which leads to isostatic adjustment and therefore an uplift of the bedrock elevation. This mechanism partly counteracts the decrease in ice surface elevation and thus mitigates further increase in temperature. The timescale of this feedback loop depends on the rate of ice retreat and on the viscosity of the upper Earth mantle.

melt rates. The GIA feedback is represented by the Lingle-Clark model, a generalization of the flat earth Elastic Lithosphere Relaxing Asthenosphere (ELRA) model (Bueler et al., 2007). The Lingle-Clark model accounts for non-local effects and different relaxation times depending on the spatial extent of the perturbation. We explore the parametric uncertainty range by varying the key parameters: asthenosphere viscosity for the bedrock uplift and the atmospheric lapse-rate for the melt-elevation feedback.

We use the Parallel Ice Sheet Model (PISM) ~~(the PISM authors, 2018; Bueler and Brown, 2009)~~ (Khroulev and the PISM authors, 2021; coupled to the Lingle-Clark solid-Earth model (Bueler et al., 2007) in order to explore the interaction between the self-amplifying and the dampening feedback. The models and the experimental design are presented in Section 2. The warming experiments use an idealized temperature forcing and are analyzed in Section 3, followed by a discussion in Section 4.

2 Methods

2.1 Numerical modeling

2.1.1 Ice-sheet dynamics with the Parallel Ice Sheet Model PISM

The Parallel Ice Sheet Model, PISM is a thermomechanically coupled finite difference ice-sheet model which combines the shallow-ice approximation (SIA) in regions of slow-flowing ice and the shallow-shelf approximation (SSA) of the Stokes flow stress balance in ice streams and ice shelves (Bueler and Brown, 2009; Winkelmann et al., 2011; the PISM authors, 2018). The internal deformation of ice is described by Glen's flow law, here the flow exponents $n_{\mathrm{SSA}} = 3$ and $n_{\mathrm{SIA}} = 3$ are used. We use the enhancement factors $E_{\mathrm{SSA}} = 1$ and $E_{\mathrm{SIA}} = 1.5$ for the SSA and the SIA stress balance respectively. Different enhancement factors of the shallow ice and the shallow shelf approximations of the stress balance can be used to reflect anisotropy of the ice, as shown by Ma et al. (2010). Aschwanden et al. (2016) used in their high resolution simulations $E_{\mathrm{SSA}} = 1$ and $E_{\mathrm{SIA}} = 1.25$, as it provided good agreement with observed flow speeds.

The sliding is described by a pseudo-plastic power law, relating the basal stress τ_b to the yield stress τ_c as

$$\tau_b = -\tau_c \frac{\mathbf{u}}{u_{\mathrm{threshold}}^q |\mathbf{u}|^{1-q}} \tag{1}$$

, with the sliding velocity $\mathbf{u}$, the sliding exponent $q = 0.6$ and the threshold velocity $u_{\mathrm{threshold}} = 100\,\mathrm{m/yr}$. The yield stress is determined from parameterized till material properties and the effective pressure of the saturated till via the Mohr-Coulomb criterion (Bueler and van Pelt, 2015)~~.~~:

$$\tau_c = (\tan\phi) N_{\mathrm{till}} \tag{2}$$

with the till friction angle ϕ, linearly interpolated at the beginning of the run from the bedrock topography between $\phi_{\mathrm{min}} = 5°$ and $\phi_{\mathrm{max}} = 40°$ between bedrock elevations of -700 m and 700 m. The effective pressure on the till N_{till} is determined from the ice overburden pressure and the till saturation as described in Bueler and van Pelt (2015).

2.1.2 Earth deformation model

While global GIA models with sea-level coupling are available, to our knowledge no coupling efforts between ice-dynamics and solid-Earth models have been undertaken for the Greenland Ice Sheet specifically. Here, the deformation of the bedrock in response to changing ice load is described with the Lingle-Clark (LC) model (Lingle and Clark, 1985; Bueler et al., 2007), incorporated as solid-earth module in PISM. In this model the response time of the bed topography depends on the wavelength of the load perturbation for a given asthenosphere viscosity (Bueler et al., 2007). The LC model uses two layers to model the solid earth: the viscous mantle is approximated by a half space of viscosity $\cancel{\nu}$ η and density ρ_r, complemented by an elastic layer of flexural rigidity D describing the lithosphere. The response of the elastic lithosphere happens instantaneously, while the response time of the viscous mantle lies between decades and tens of millennia, depending on both, the viscosity of the mantle and the wavelength of the change in load. While the Lingle-Clark model is not considering local changes to viscosity or lithosphere thickness (Milne et al., 2018; Mordret, 2018; Khan et al., 2016) and approximates the earth as a half space, the relatively small spatial extent of the simulation region allows for such an approximation.

The resulting partial differential equation for vertical displacement u of the bedrock can be described by

$$2\nu\eta|\nabla|\frac{\partial u}{\partial t} + \rho_r g u + D\nabla^4 u = \sigma_{zz}. \tag{3}$$

with g being the gravitational acceleration of the earth and σ_{zz} the ice load force per unit area (Bueler et al., 2007).

Here the flexural rigidity D is assumed to be 5×10^{24} Nm, assuming a thickness of 88 km for the elastic plate lithosphere (Bueler et al., 2007). The mantle density ρ_r is approximated with $3300\,\mathrm{kg/m^3}$.

Following Bueler et al. (2007), Eq. (14), we show how the spectrum of the relaxation time of the solid Earth model depends on the wavelength of the ice load change and how this relationship changes for different mantle viscosities and lithosphere flexural rigidities in Fig. A1. In general high mantle viscosities shift the spectrum to higher relaxation times, the maximal relaxation time increases by more than two orders of magnitude, from approx 100 yrs to approx 50000 yrs, while the thickness of the lithosphere has a less strong effect on the relaxation times spectrum.

2.1.3 Climatic mass balance and temperature forcing

The climatic mass balance in PISM is computed with the positive degree day (PDD) model from 2m-air temperature and precipitation given as inputs (Braithwaite, 1995). Here we use a yearly cycle of monthly averages from 1958 to 1967 of the outputs of the regional climate model RACMO v2.3 (Noël et al., 2019) in order to mimic preindustrial climate. The warming is implemented as a spatially uniform instantaneous shift in temperature. The temperature forcing itself has a yearly cycle, with the temperature shift in winter being twice as high as in summer. This corresponds to an average Arctic amplification of 150 % (see also Robinson et al. (2012)).

The PDD method uses the spatially uniform standard deviation $\sigma = 4.23$, the melt factors for snow and for ice $m_i = 8\,\mathrm{mmK^{-1}day^{-1}}, m_s = 3\,\mathrm{mmK^{-1}day^{-1}}$ (PISM default) respectively. The melt-elevation feedback is approximated by an atmospheric temperature lapse rate Γ, so that local changes in the ice-sheet topography alter the temperature as

$$T_{ij} = T_{ij,\text{input}} - \Gamma\cdot\Delta h_{ij}, \tag{4}$$

with T_{ij} being the effective temperature at grid cell i,j feeding into the PDD model. $T_{ij,\text{input}}$ is the temperature at i,j given by the input, without any lapse rate correction, Γ is a spatially constant air-temperature lapse rate. $\Delta h_{i,j} = h_{t,ij} - h_{0,ij}$ is the local difference in surface elevation at i,j at time t, compared to a reference topography h_0. Here we use the initial state for h_0. The value of the lapse rate Γ, and thereby the strength of the melt-elevation feedback, is varied between 5 K/km and 7 K/km in the experiments.

The yearly precipitation cycle remains ~~prescribed~~fixed and does not scale with temperature, the local temperature affects how much of the precipitation is perceived as snow and therefore adds to the accumulation: at a temperature above 2°C, all precipitation is perceived as rain, below 0°C all is perceived as snow, with a linear interpolation between the two states ~~.~~(the default in PISM). The climatic mass balance is adjusted via a flux correction in the regions which are ice-free in present-day to keep them ice-free. How variations in these three assumptions affect the results is discussed in Sec. 4.3.

2.2 Experimental design

Here we use a spatial resolution in x and y direction of 15 km in order to do many simulations over 0.5 million years. The spatial resolution in z-direction is quadratically decreasing from 36 m in the cell closest to the bedrock to 230 m in the top grid cell of the simulation box (at 4000 m above bedrock).

The temperature forcing is a spatially uniform step forcing, which is applied from $t = 0$ over the whole simulation time. Additional local temperature changes happen due to the atmospheric temperature lapse rate, as shown above. We explore different values for the atmospheric lapse rate in order to estimate the response of the system to changes in the strength of the melt-elevation feedback.

The ice-ocean interaction is modeled via PICO, with ocean temperatures and salinities taken from the World Ocean Atlas version 2 (Zweng et al., 2018; Locarnini et al., 2019) ~~. Temperatures and salinities are averaged at bottom depth over the~~ and remapped onto the simulation grid of 15 km horizontal resolution. PICO used one average value of temperature and salinity per extended drainage sector (for the extended ~~drainage sectors of the GrIS. For the extended~~ sectors, the drainage sectors of Rignot and Mouginot (2012) are extended linearly into the ocean~~. The~~), even as the ice sheet advances or retreats. The averages are taken at bottom depth over the continental shelf. The warming signal at depth generally stabilizes at lower levels than the atmospheric or sea surface warming, here we assume that only 70% of atmospheric warming reaches the ocean ground (see also Albrecht et al. (2020)). However, only less than 0.2% of the Greenland Ice Sheet area are made up of floating ice tongues and the ocean forcing is not transferred to the ice fronts of grounded tidewater glaciers, so the ice-ocean interaction is not the main driver in this simulation setup.

Calving is modeled as a combination of eigencalving (Winkelmann et al., 2011; Levermann et al., 2012) and von-Mises calving (Morlighem et al., 2016) with constant calving parameters. In addition a maximal floating ice thickness of 50 m is imposed.

2.2.1 Initial state

The initial state is in equilibrium for constant climate conditions. The misfits of the initial state compared to observed velocities (Joughin et al., 2018) and thicknesses (Morlighem et al., 2017) and to modelled climatic mass balance (Noël et al., 2019) are shown in the Supplementary Material in Figures S1, S2 and S3. All simulations are run at a spatial horizontal resolution of 15 km. The basic dynamics of the melt-elevation feedback and the GIA feedback are well captured at this resolution, which allows to explore the parameter space effectively. However, a lot of features of the complex flow of outlet glaciers are not captured at this resolution.

2.2.2 Choice of model parameters

We chose to vary along three main parameters. On the one hand, we vary the strength of the melt-elevation feedback by varying the atmospheric temperature lapse rate Γ between 5 K/km and 7 K/km. Many ice-sheet models use the free air moist adiabatic lapse rate (MALR), which ranges between 6-7 K/km (Gardner et al., 2009) for high humidity, but assumed to be higher in cold

Table 1. Parameters used in experiments

Name	Parameter	Value
ΔT	Temperature increase	~~1.5, 2, 3~~[1.5, 2, 3] K
Γ	Atmospheric temperature lapse rate	~~5 – 7~~[5, 5.5, 6, 6.5, 7] K/km
~~ν~~ η	Mantle viscosity	~~$1\times10^{-19} - \times10^{21}$~~ $[1\times10^{19}, 1\times10^{20}, 1\times10^{21}, 5\times10^{21}]$ $\mathrm{Pa\cdot s}$

temperatures when the air is dry (Fausto et al., 2009). However, the mean slope lapse rates measured in Greenland and on other ice caps in the Arctic tend to be lower than the MALR and show seasonal variation (Fausto et al., 2009; Gardner et al., 2009; Steffen and Box, 2001; Hanna et al., 2005). By using spatially and temporally constant lapse rates between 5-7 K/km we try to cover a realistic range in lapse rates.

In addition, the response time and strength of the bedrock to changes in ice load is determined by the mantle viscosity ~~ν~~η, varied between 1×10^{19} $\mathrm{Pa\cdot s}$ and 5×10^{21} $\mathrm{Pa\cdot s}$. This range is larger than the values of the upper mantle viscosity given in the literature, which still range over more than two order of magnitude over Greenland alone, usually around $1\cdot10^{20}$ $\mathrm{Pa\cdot s}$ to $5\cdot10^{21}$ $\mathrm{Pa\cdot s}$, but local values from $1\cdot10^{18}$ $\mathrm{Pa\cdot s}$ to $1\cdot10^{23}$ $\mathrm{Pa\cdot s}$ cannot be ruled out ~~(Tosi et al., 2005; **?**; Mordret, 2018; Khan et al., 2016; Wahr et al., 200~~ (Tosi et al., 2005; Adhikari et al., 2021; Mordret, 2018; Khan et al., 2016; Wahr et al., 2001; Peltier and Drummong, 2008; Larour et al., 2 . Ice retreat itself is affected by the temperature anomaly, here varied between 1.5 K and 3.0 K global warming (note the arctic amplification of 150 % leading to higher local temperature anomalies).

3 Results

Here, we analyze how the strengths of the melt-elevation feedback and the GIA feedback influence the long term dynamics of the Greenland Ice Sheet in PISM simulations.

3.1 Temporal evolution of ice volume under temperature forcing depending on atmospheric lapse rate and mantle viscosity

The ice losses in simulations with applied warming are affected by both ~~,~~ the amplifying melt-elevation feedback and the mitigating GIA feedback. The interaction of both feedbacks allows for a variety of dynamic regimes, depending on the amount of warming on the one hand and the parameters describing the feedback strength on the other hand.

At a given temperature anomaly (here $\Delta T = 2\,\mathrm{K}$) and a given mantle viscosity (here ~~$\nu = 1\times10^{21}$~~$\eta = 1\times10^{21}$ $\mathrm{Pa\cdot s}$), both, the rate and magnitude of the initial volume loss increase with increasing air temperature lapse rate, i.e. a stronger melt-elevation feedback (see Figure 2 (A)). With a lapse rate of $\Gamma = 5$ K/km, at the low end of the tested range, ~~a~~ an incomplete recovery after an initial ice loss is observed, the ice sheet loses approx 1.5 m sea-level equivalent in volume, before stabilizing at 6 m SLE after approx. 50 kyrs (1 m SLE corresponds to approx. 361 800 Gt of ice). With an increasing lapse rate and thereby increasing strength of the melt–elevation feedback the ice volume may still recover after a stronger initial loss. At sufficiently

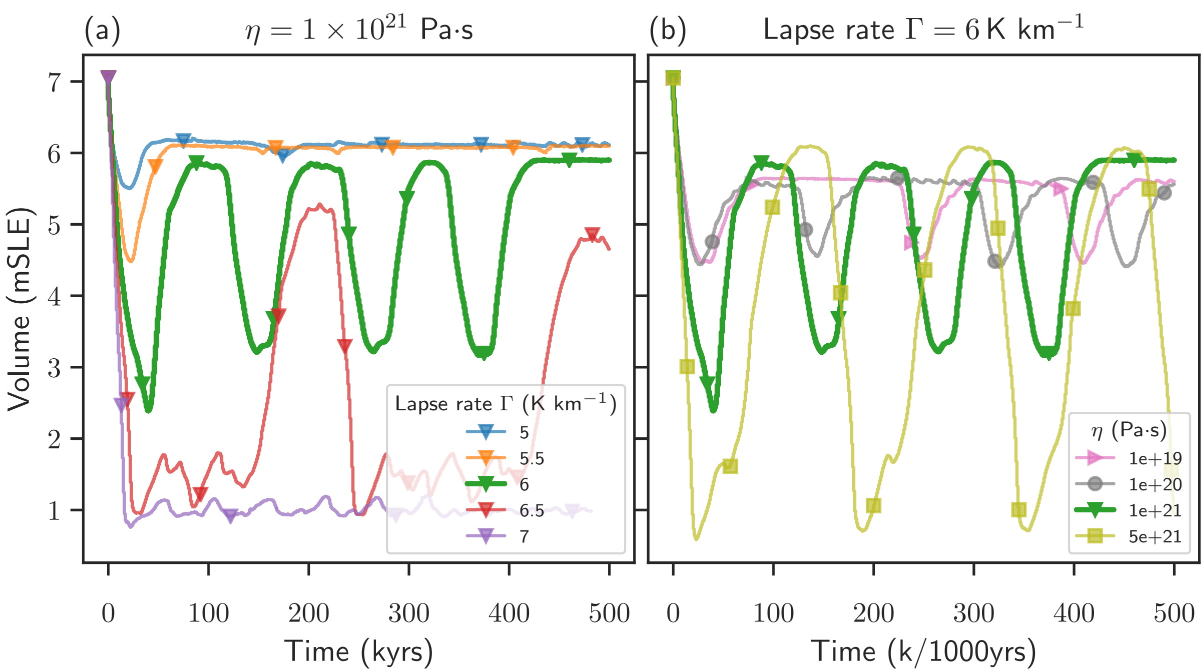

Figure 2. Temporal evolution of Greenland Ice Sheet volume at a temperature anomaly of $\Delta T = 2$K. Depending on the atmospheric temperature lapse rate (between 5 and 7 K/km) **(A)** and on the mantle viscosity (between 1×10^{19} and 5×10^{21} Pa·s) (B) distinct regimes of dynamic responses are observed, including incomplete recovery, quasi-periodic oscillations and permanent loss of ice volume.

high lapse rates the recovered state is not stable on long time scales. A self-sustained oscillation of repeated ice losses and gains is observed for $\Gamma = 6$ K/km with an oscillation time scale of approx. 109 kyrs. Increasing the lapse rate even further, to $\Gamma = 7$ K/km does not allow the ice to recover at all, the ice volume is permanently lost.

Here, depending on the value of the lapse rate Γ three qualitatively different response regimes are observed, (i) incomplete recovery, (ii) self-sustained quasi-periodic oscillation, and (iii) permanent ice loss.

In contrast a constant lapse rate of Γ =6 K/km, a warming of $\Delta T = 2$K and varying mantle viscosities between ~~$\nu = 1 \times 10^{19} - 5 \times 10^{21}$~~ η to self-sustained oscillations (ii) in the ice sheet volume independently of the value of the mantle viscosity (see Figure 2 (B)). The variations in mantle viscosity do not change the dynamic regime qualitatively, they affect however the time scale and the amplitude of the observed oscillations. Large values for the mantle viscosity are associated with a smaller response time scale of the GIA and thereby allow for larger initial ice losses and large amplitudes of oscillation. The amplitude, here taken as the difference between the maximal and the minimal volume after an initial ice loss, increases from 1.2 m sea level equivalent to 5.5 m sea level equivalent by increasing the mantle viscosity from ~~1e+19 Pa·s to 5e+21 Pa·s.~~ 1×10^{19} Pa·s to 5×10^{21} Pa·s. 1 m sea level equivalent corresponds to approx. 361800 Gt of ice

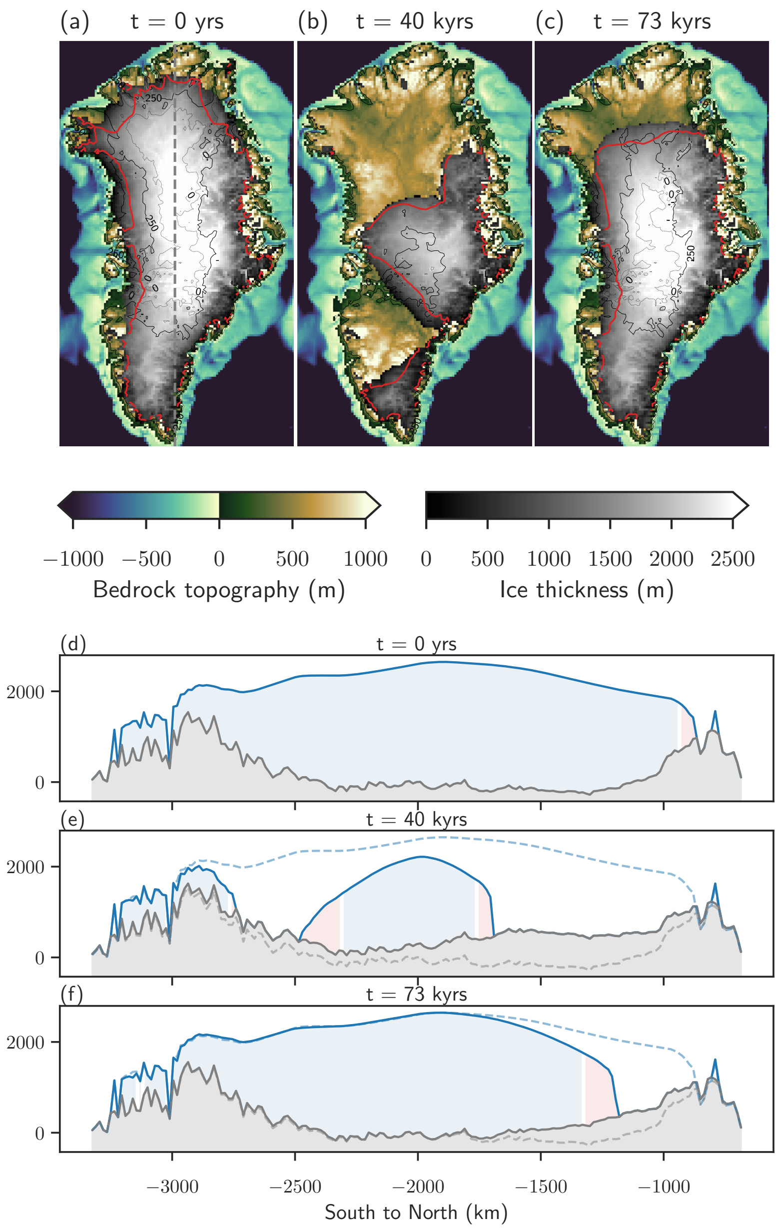

Figure 3. Spatial distribution of ice thickness at a temperature anomaly of $\Delta T = 2$K for the parameters ~~$\nu = 1 \times 10^{21}$~~ $\eta = 1 \times 10^{21}$ Pa$\cdot$s, $\Gamma = 6\,\mathrm{K/km}$. Maps and cross-sections of the bedrock topography and ice thickness show the initial state at the start of the simulation (A,D), the state with minimal volume after 40 kyrs (B,E) and the recovered state after 73 kyrs (C,F). The red outline and the red shaded areas indicate the ablation regions. The dashed lines in (E) and (F) show the initial topography of the ice sheet.

~~The observed oscillations in ice sheet volume (regime ii) are not perfectly periodical, therefore the concepts of periodicity or frequency cannot be directly applied. This framing would require that the physical state of the ice sheet, regarding not only its volume but also spatially resolved variables like thickness distribution, velocity fields, the state of the solid earth and the climate, return to exactly the same state after one oscillation period. Instead we here use a power spectrum analysis to estimate the characteristic time of oscillation. The oscillation times in this study vary between 79 kyrs (for $\Delta T = 3\,\mathrm{K}$, $\nu = 1 \cdot 10^{21}$ and $\Gamma = 5.5$ K/km) and 250 kyrs (for $\Delta T = 2\,\mathrm{K}$, $\nu = 1 \cdot 10^{21}$ and $\Gamma = 6.5$ K/km). An even longer oscillation time of 333 kyrs is found for $\Delta T = 1.5\,\mathrm{K}$, $\nu = 1 \cdot 10^{19}$ and $\Gamma = 6.0$ K/km, it is however seemingly an outlier: the ice sheet volume seems to recover and reach a permanently stable plateau, but after 250 kyrs a decline in ice-sheet volume is re-initiated. The oscillation times do not seem to show a clear dependence on the values for warming, lapse rate or mantle viscosity.~~

The spatial configuration of the ice thickness, the bedrock topography and the equilibrium line, separating the accumulation from the ablation region in response to warming is visualized for one example simulation in the oscillation regime (ii), with the parameters $\Delta T = 2\,\mathrm{K}$, ~~$\nu = 1 \times 10^{21}$~~ $\eta = 1 \times 10^{21}$ $\mathrm{Pa \cdot s}$ and $\Gamma = 6\,\mathrm{K/km}$. We choose three points in time, representing the initial state, the state with minimal ice volume and the oscillation maximum, a recovered state which is unstable on long time scales (see Figure 3). The time evolution of the volume is depicted by the thick green curve in Figure 2. During the retreat phase, the mass loss of the ice is initiated from the north of the ice sheet. The area and volume of the ice sheet decrease and reach a minimal value after approx. 40 kyrs, with a remaining ice dome over central Greenland and a second smaller ice patch over the southern tip of Greenland. This ice loss is accompanied by an uplift of the bedrock which is most prominent in areas with complete ice loss. The maximal ice thickness decreases from 2940 m to 2270 m in the minimal volume state, attained in the ~~2astern~~ Eastern region of the ice larger ice dome. The maximal bedrock uplift of 740 m is found in the northern region where the most ice is lost. The minimal state is also characterized by an increase in relative ablation area, 29% compared to 24% in the initial state. The maximal relative ablation area of 31% is reached approx. 500 years before the minimum of the volume is reached. Eventually, the accumulation area expands and allows the ice sheet to regrow. However, the maximally recovered ice sheet differs from the initial state in area, thickness distribution, accumulation area, and bedrock topography (see Figs. 3 C and F). In particular the ice sheet extends much less to the north than in the initial state. The precipitation field is assumed to be constant in time, there is no feedback between the ice sheet topography and the precipitation pattern.

3.2 Competing positive melt-elevation and negative GIA feedbacks

Here we explore the competing feedbacks by varying the parameters, which determine the relative strengths of the involved feedbacks, simultaneously.

3.2.1 Dynamic regimes

To gain a better understanding of the dynamic regimes of the GrIS we tested the long-term response of the ice-sheet volume to warming in the full-factorial parameter space $\Delta T, \Gamma$ and ~~ν~~ η with values given in Table 1. As stated above in Section 3.1 four qualitatively different response regimes can be distinguished: ~~(o) Direct stabilization into a new equilibrium state which preserves 90% or more of the initial ice volume. (i) Recovery~~ (i) incomplete recovery to a stable state after an initial ice loss.

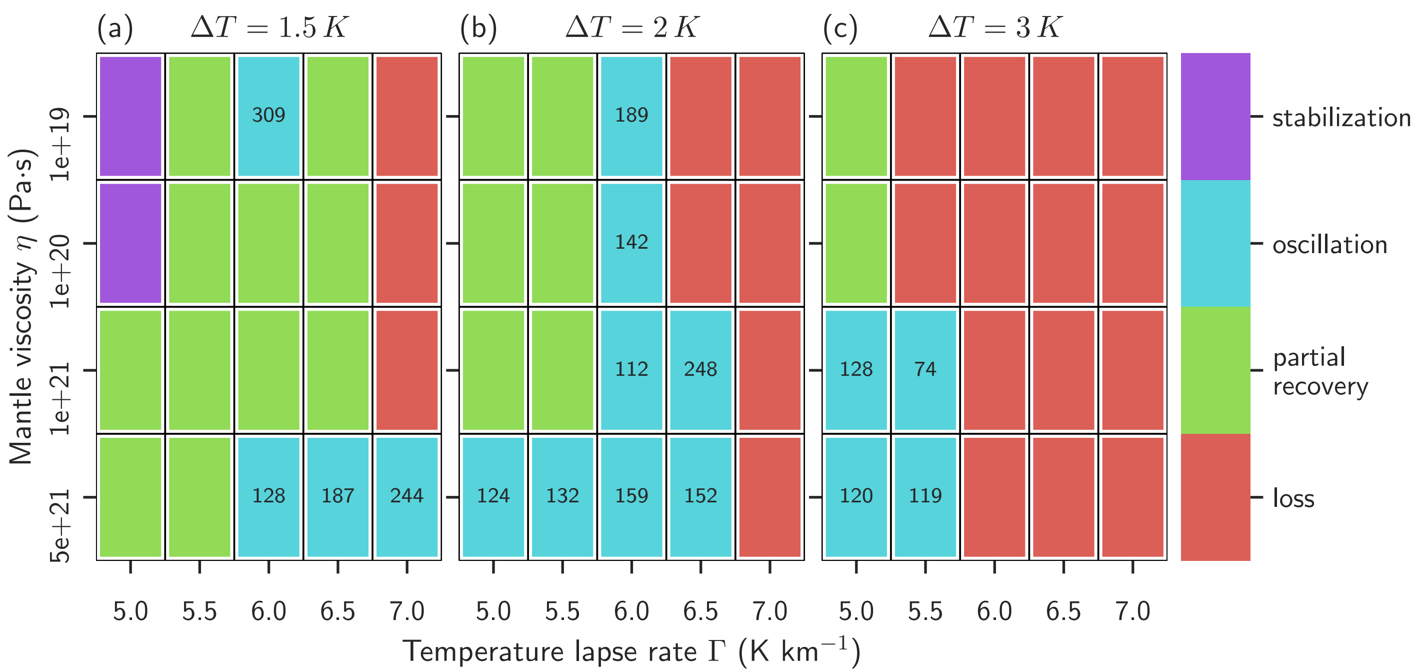

Figure 4. Dynamical regimes of Greenland ice sheet evolution for three different warming temperatures, $\Delta T = 1.5\,\mathrm{K}$, 2 K, and 3 K. The evolution regime of the Greenland Ice Sheet volume is indicated by the color code. Purple indicates immediate stabilization to a stable state, which preserves more than 90 % of the initial ice sheet volume, without passing a minimum. Green indicates, that the ice sheet volume recovers permanently after passing a minimum first. Blue indicates, that the ice sheet volume does not recover permanently, but shows self-sustained oscillations on a long time scale instead. Red indicates a permanent loss of ice sheet volume. The numbers in the cyan tiles show the approximate oscillation times.

(ii) Self-sustained qasi-periodic oscillations and (iii) Irreversible loss of a large portion of the ice ~~.~~ or (iv) direct stabilization into a new equilibrium state which preserves 90% or more of the initial ice volume. Note that only oscillations with a minimal amplitude of 0.5 mSLE are included in the oscillating regime.

With increasing temperature anomalies ΔT a larger portion of the parameter space experiences irreversible ice loss (iii) (Figure 4). For a warming temperature of 3 K for example, irreversible ice loss is observed for lapse rates greater or equal than 6 K/km for all mantle viscositites and for 5.5 K/km for mantle viscosities lower or equal to 1e+20 Pa·s.

Moreover, increasing temperature lapse rate promotes irreversible ice loss, for instance at $\Gamma = 7$ K/km, irreversible ice loss occurs for warming temperatures of 2 K or warmer, regardless of the choice for the mantle viscosity (see Figure 4) and also for most simulations with $\Delta T = 1.5\,\mathrm{K}$.

Direct stabilization without going though a minimum (o) is only realized for the lowest temperature anomaly $\Delta T = 1.5\,\mathrm{K}$ and at the lowest lapse rate $\Gamma = 5$ K. While incomplete recovery or stabilization are the most prevalent regimes for low warming temperatures (1.5 K) in the tested parameters space, the oscillatory regime is realized most often at temperature anomalies of

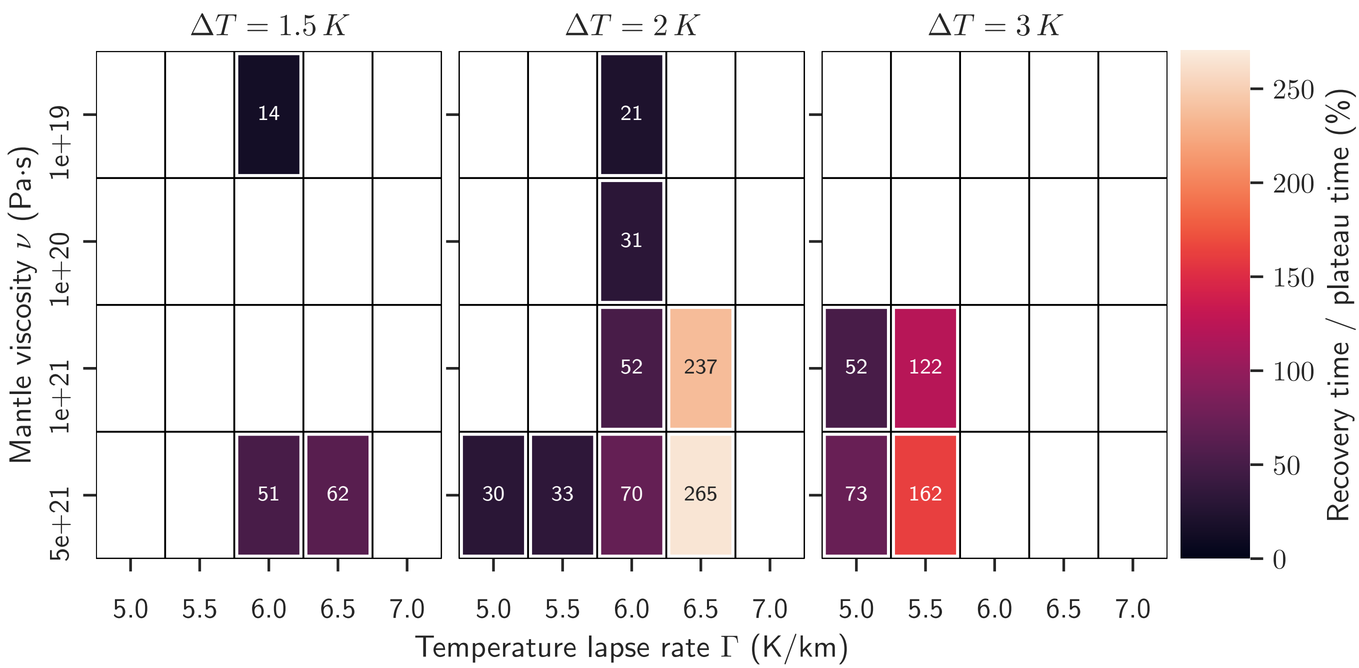

Figure 5. **Ratio of recovery time vs. plateau time** for three different warming temperatures, $\Delta T = 1.5\,\mathrm{K}$, $2\,\mathrm{K}$, and $3\,\mathrm{K}$. Measure for how long the lower half of the oscillation is compared to the upper half. A ratio of 1 would signify a perfectly symmetric oscillation, the lower the number, the more time is spent in a recovered regime (ice volume > average of minimal and maximal oscillation volume), and the higher the number the more time is spent at low ice volumes (ice volume < average of minimal and maximal oscillation volume).

2 K. High mantle viscosities promote oscillations of the ice sheet volume as they lead to a slower response of the bedrock to changes in ice loss and thereby allow for a stronger retreat phase and thereby a faster initial ice loss with warming, as seen in Fig. 2. On the other hand, the more pronounced retreat initiates a strong bedrock response which supports the recovery. However, the recovered state is not in equilibrium with the bedrock, and thereby a self-sustained oscillation can be triggered.

3.2.2 ~~Minimum and maximum ice volume for recovery or~~ Time scales in the oscillation ~~regimes~~regime

The observed oscillations in ice sheet volume (regime iii) are not perfectly periodical, therefore the concepts of periodicity or frequency cannot be directly applied. This framing would require that the physical state of the ice sheet, regarding not only its volume but also spatially resolved variables like thickness distribution, velocity fields, the state of the solid earth and the climate, return to exactly the same state after one oscillation period. Instead we here estimate the characteristic duration of the oscillation via a simple algorithm: first we identify the minimal and maximal volume of the oscillation, and the center of both. As the oscillation is not symmetric, the time-average of the volume would be not centered between the minimum and the maximum. In a next step we measure the time between two intersections of the time series with the central oscillation volume, which would correspond to a half oscillation, if those were perfectly symmetric and periodic. The average time between one intersection and the next but one corresponds to the oscillation time. As only a few oscillation periods fit in to the simulation time of 500 kyrs, a thorough statistical analysis can not be performed. Note that the uncertainty arising from choosing the central volume between the minimal and the maximal volume, rather than a weighted average, are much less than the uncertainty due to the imperfect periodicity, as they amount to less than 1% in most cases and to about 2.5% in the worst case.

The oscillation times, as shown in Fig. 4, in this study vary between 79 kyrs (for $\Delta T = 3\,\mathrm{K}$, $\eta = 1 \cdot 10^{21}\,\mathrm{Pa \cdot s}$ and $\Gamma = 5.5\,\mathrm{K/km}$) and 250 kyrs (for $\Delta T = 2\,\mathrm{K}$, $\eta = 1 \cdot 10^{21}\,\mathrm{Pa \cdot s}$ and $\Gamma = 6.5\,\mathrm{K/km}$). An even longer oscillation time of 309 kyrs is found for $\Delta T = 1.5\,\mathrm{K}$, $\eta = 1 \cdot 10^{19}\,\mathrm{Pa \cdot s}$ and $\Gamma = 6.0\,\mathrm{K/km}$, which is however strongly asymmetric: the ice sheet volume seems to recover and reach a permanently stable plateau, but after approx 250 kyrs a decline in ice-sheet volume is re-initiated. The oscillation times do not seem to show a clear dependence on the values for warming, lapse rate or mantle viscosity. The oscillation time is governed by a more complex interplay of the dynamics: time scale and depth of the initial deglaciation, level of maximally recovered volume, stability of the plateau between ice losses. The analysis method described above, allows to distinguish between the average time for the lower half of the oscillation ("recovery time") and the upper half of the oscillation ("plateau time"). We find that generally the recovery time is shorter than the plateau time, 10% in the case of $\Delta T = 1.5\,\mathrm{K}$, $\eta = 1 \cdot 10^{19}\,\mathrm{Pa \cdot s}$ and $\Gamma = 6.0\,\mathrm{K/km}$ (oscillation time 309 kyrs). This ratio increases with temperature forcing ΔT, with the mantle viscosity η, and most strongly with the lapse rate Γ up to 265% for the parameter combination of $\Delta T = 2\,\mathrm{K}$, $\eta = 5 \cdot 10^{21}\,\mathrm{Pa \cdot s}$ and $\Gamma = 6.5\,\mathrm{K/km}$ (see Fig. 5). The smaller this ratio, the more stable the partially recovered state of the ice sheet.

3.2.3 Minimum and maximum ice volume for incomplete recovery or oscillation regimes

The long-term response of the Greenland Ice Sheet volume to temperature anomalies can be characterized by the minimal and maximal long-term volume, defined as the minimal and maximal volume attained after passing an initial minimum. In the dynamic regimes of stabilization, incomplete recovery, and permanent ice loss the minimal and maximal long-term volumes are therefore almost identical. The absolute values of the minimal and maximal long-term volume determine how much ice is lost and the difference between them shows how large the amplitude of the oscillation is. The minimal and maximal long-term volumes are visualized in Figure 6. Here, two values are shown for each parameter combination. The upper pixels represent the maximum long-term volume, while the lower pixel represents the minimum long-term volume. A comparison to the regime shown in Figure 4 reveals that both volumes are high if the ice volume is stabilized directly or recovers, and both volumes are low if the ice is permanently lost. Oscillations are characterized by a significant difference between the minimal and maximal long-term volume. Generally, the absolute values for either stabilized, oscillating or lost volume decrease with increasing warming. The amplitude of oscillations is highest for high mantle viscosities, since the slow response time associated with high mantle viscosities allows for more ice loss but also for a stronger recovery.

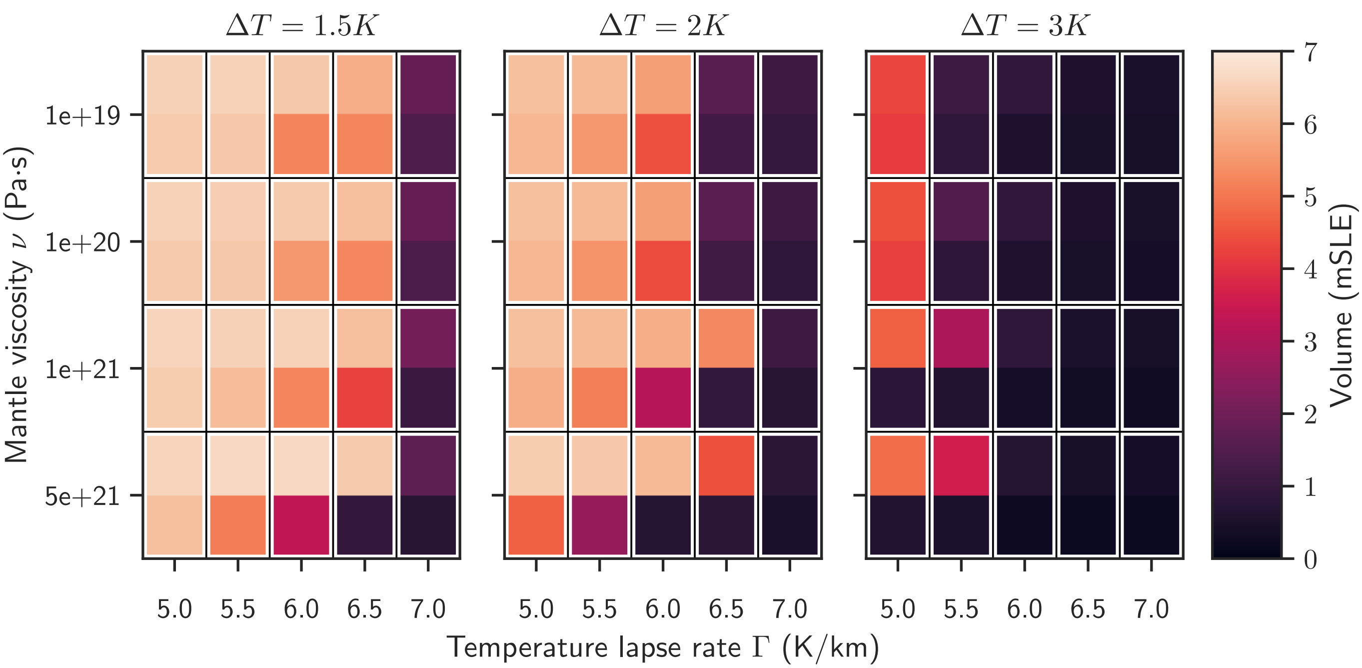

Figure 6. Minimal and maximal volume after initial ice loss for three different warming temperatures, $\Delta T = 1.5\,\mathrm{K}$, $2\,\mathrm{K}$, and $3\,\mathrm{K}$. Two pixels represent the minimal (lower) and the maximal (upper) long-term volume for each parameter combinations. The minimal and maximal long-term volume is defined by the minimum or the maximum of the volume after passing the initial minimum. A significant difference between the minimal and the maximal volume indicates oscillation.

3.3 State space trajectories

Here we analyze the different dynamic regimes of the Greenland Ice Sheet via their trajectories through state space. The full state space of an ice sheet has a very high dimensionality and even with the simplifications made by numerical modelling, the full state space remains inaccessible. Here we choose the projection of the state to three state variables: ~~The~~ the temporal evolution of the average topography altitude of the glaciated areas on the one hand and the ablation or accumulation area of the ice sheet on the other hand. In both cases the variables are averaged over glaciated areas rather than over a fixed area (e.g. the initial ice sheet area), because this is where they affect the ice sheet. For instance the bedrock uplift in a region which has (permanently) lost its ice does not take part in the feedback as described in Fig. 1. The average topography altitude can change either via glacial isostatic adjustment while the ice sheet area is constant or by changing the ice sheet area at constant topography or a combination of those two processes. The ablation or accumulation area can either change though changes in the ice-sheet area at constant climatic mass balance or via changing the climatic mass balance but keeping the ice-sheet area constant (or a combination of those two processes).

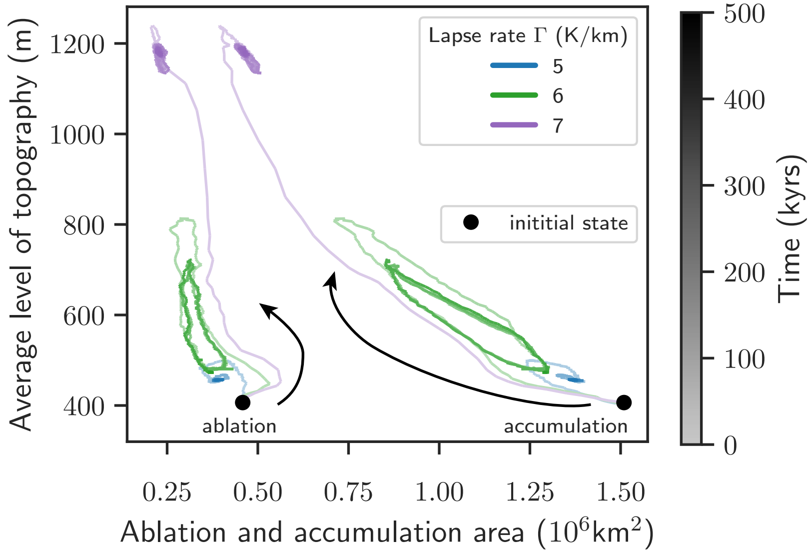

Figure 7. State space trajectories for different regimes for the three different lapse rates $\Gamma = [5, 6, 7]$ K/km. The curves represent the average height of the bedrock topography vs. the ablation and the accumulation area. Blue: Lapse rate $\Gamma = 5$ K/km, incomplete recovery of the ice volume. Green: Lapse rate $\Gamma = 6$ K/km, oscillation of the ice volume. Purple: Lapse rate $\Gamma = 7$ K/km, irreversible loss of the ice volume. The color code corresponds to Figure 2 a, that is the temperature forcing is $\Delta T = 2$ K and the mantle viscosity is $\eta = 1 \times 10^{21}$ Pa$\cdot$s. The color shading represents time, as indicated by the color bar on the right side. The average bedrock and the accumulation and ablation area of the initial state are represented by the black marker.

We interpret the topography altitude as a measure of the GIA feedback and the accumulation and ablation area as a measure for the climatic processes.

We can distinguish three different "phase space trajectories" for the different regimes: incomplete recovery after an initial ice loss (i), oscillation (ii) and ice-sheet collapse (iii). All of the simulations shown here are at $\Delta T = 2$ K and with the mantle viscosity of $\cancel{\nu = 1 \times 10^{21}}$ $\eta = 1 \times 10^{21}$ Pa$\cdot$s.

For $\Gamma = 5$ K/km (blue curves in Figure 2 (A) and Figure 7), the ice sheet is in the incomplete recovery regime. Both ~~,~~ the accumulation / ablation areas and the average topography diverge the least from the starting point compared to the other simulations. The trajectories for both accumulation and ablation area spiral quickly into a fixed point. The trajectory for the ablation area follows a counterclockwise spiral while the trajectory for the accumulation area follows a clockwise spiral. ~~The trajectory for the ablation area starts out almost vertically upwards, only little change in the ablation area is observed. The accumulation however shrinks while the bedrock elevation rises. The turning point is characterized by a shrinking ablation area, a rising accumulation area and a depression in bedrock elevation.~~ Here, changes in accumulation area seem to be more important than the changes in the ablation area and to drive the dynamics. ~~Moreover, the ablation and the accumulation area do not seem to be independent, they show, as expected, an anticorrelation.~~

For $\Gamma = 6$ K/km (green curves in Figure 2 (A) and Figure 7) the ice sheet is in the oscillation regime. The trajectories spiral into a closed loop rather than a fixed point, which is characteristic for limit-cycles and non-linear oscillators. Again, the trajectory with the ablation area goes counter-clockwise while the trajectory for the accumulation area goes clockwise. In absolute terms the accumulation area changes more drastically than the ablation area during one cycle, an indication that the change in accumulation area drives the ice loss. ~~The total change in ice-sheet area is reflected through the sum of ablation and accumulation area. Even though the trajectories form a closed loop in this simulation~~Even though these trajectories form closed loops, there is no perfect periodicity ~~. In particular the first loop in~~ in the beginning, as the first loop of the trajectory is larger than the subsequent ~~quasi-periodic behavior~~following ones.

The atmospheric lapse rate of $\Gamma = 7$ K/km (purple curves in Figure 2 (A) and Figure 7) leads to irreversible ice-sheet collapse under these parameters. The trajectories approach again a fixed point. Both the accumulation and the ablation area are smallest, compared to the other two lapse rate simulations, indicating that the total area of the ice sheet is also small. Again, the absolute change in accumulation area is more drastic than the change in ablation area ~~. In addition,~~ and the change in average level of bedrock topography is highest. As indicated beforehand, this is both related to the bedrock uplift (most ice loss allows for the strongest uplift) as well as to the fact that the remaining ice retreats to high altitude mountainous areas with a lot of precipitation and comparatively low temperatures.

~~The trajectories of the different regimes do not intersect, suggesting that the phase space is well represented.~~

4 Discussion

~~In this manuscript, we show how the negative glacial isostatic adjustment feedback (connecting ice sheet and solid Earth) can counteract the positive melt-elevation feedback (connecting atmosphere and ice sheet) and thus the long-term ice loss of the Greenland Ice Sheet under warming temperatures. The interaction of both feedbacks determines the dynamic regime and the stability of the Greenland Ice Sheet. Depending on the individual feedback strengths, expressed through mantle viscosity and atmospheric temperature lapse rate respectively, we find distinct regimes for the evolution of the ice volume: the transition to a new steady state, recovery after an initial ice loss, self-sustained quasi-periodic oscillations or irreversible ice-sheet collapse. Although it is not explicitly studied here, drastic changes in the ice volume of the Greenland Ice Sheet would have implications for the global earth system via global sea level rise, changes in the planetary albedo, and changes in the atmospheric and oceanic circulation patterns as the Jetstream or the Atlantic Meridional Overturning Circulation (AMOC).~~

~~The strength of the melt-elevation feedback impacts the vulnerability of the Greenland Ice Sheet to temperature increases: Varying the feedback strength through the atmospheric lapse rate from 5 K/km to 7 K/km increases the probability of permanent ice loss for global mean temperature anomalies $\Delta T \geq 1.5$ K, assuming 150% of arctic amplification. Increasing the mantle viscosity from 1×10^{19} Pa·s to 5×10^{21} Pa·s increases the likelihood for self-sustained oscillations and their corresponding amplitude. The characteristic period of oscillation is in the order of 100 kyrs, which is rather independent of both, mantle viscosity or temperature lapse rate. However, in case of recovery the associated characteristic response time seems to increase with increasing lapse rates or mantle viscosities.~~

4.1 GIA feedback in different contexts

The impact of the GIA feedback on ice-sheet dynamics has been studied in different contexts. Marine terminating glaciers and ice shelves are particularly sensitive to glacial isostatic rebound, as it can influence the position of the grounding line and how exposed the ice shelf or the glacier front is to warm ocean water (Larour et al., 2019; Whitehouse et al., 2019). Observational evidence pointing to an overshoot and readvance of the grounding line in the Ross Sea, Antarctica, can be explained by the viscous response of the solid Earth to changes in ice load within a confined range of mantle viscosities (Kingslake et al., 2018). Feldmann and Levermann (2017) showed, that the complex interplay of time scales associated with the surge, buildup and stabilization feedbacks could explain Heinrich-like events.

4.2 GrIS ice volume oscillations in the context of the Earth System

While oscillations of ice volume have already been discussed in the context of marine ice sheets (Antarctic Ice Sheet, Laurentide Ice Sheet) (Bassis et al., 2017), we here find that the interaction of the melt-elevation feedback and the GIA feedback ~~alone~~ can promote an oscillatory dynamic response ~~.~~ in a mostly grounded ice sheet.

~~Hoever, small oscillations in the GrIS ice volume seem to appear in simulations with a coupled ice-sheet and regional climate model (Petrini et al., 2021). Although the oscillatory regime is not studied explicitly by Petrini et al., its appearance indicates that this dynamic regime is unlikely to be an artifact of our particular experimental design.~~

The oscillation time are of the same order of magnitude as the time scale of Earth's glaciation cycle, with a dominant period of 41 kyrs before and a period of 100 kys after the Mid-Pleistocene Transition 1.25–0.7 million years ago (Abe-Ouchi et al., 2013; Willeit et al., 2019). While the onset and the termination of glaciation are driven by changes in insolation, climate and earth surface albedo (Ganopolski and Calov, 2011) our results offer a new perspective. The identified oscillatory regime reveals a possible mode of internal climatic variability in the Earth system on time scales on the order of 100 kyrs that may be excited by or interact with orbital forcing, glacial cycles and other slow modes of variability (Ghil and Lucarini, 2020). As such, this oscillatory mode could be relevant in the long-term Earth system response (on the order of 100 kyrs) to anthropogenic carbon emissions (Talento and Ganopolski, 2021).

Our findings suggest a sequence of dynamic regimes of the Greenland Ice Sheets on the route to destabilization under global warming, within a certain range of lapse rate coefficients: from recovery, via quasi-periodic variations in ice volume to irreversible ice-sheet collapse. This transition might be similar to destabilization scenarios via oscillatory instabilities which have been revealed for other tipping elements in the climate system, such as the Atlantic Meridional Overturning Circulation (AMOC) (Alkhayuon et al., 2019). A relevant area of future research will be to develop a deeper understanding of such ice sheet destabilization routes via the concept of bifurcations (e.g., Hopf and fold bifurcations) in the context of dynamical systems. The interplay between an amplifying and a mitigating feedback contributes to our understanding of the long-term stability and the resilience of the Greenland Ice Sheet. Therefore we need to identify the most important underlying physical processes and the interactions of the feedbacks at play.

4.3 Robustness analysis

While large amplitude oscillations generated with a process based ice-sheet model have not been reported in the peer-reviewed literature, small oscillations in the GrIS ice volume seem to appear in simulations with the CISM ice-sheet model coupled to an ELRA bedrock model (Petrini et al., 2021) under constant climate. Although the oscillatory regime is not studied explicitly by Petrini et al., its appearance indicates that this dynamic regime is unlikely to be an artifact of our particular experimental design.

In addition Oerlemans (1982) found unforced oscillations in a simple ice-sheet model, including simple representations of the melt-elevation feedback (depending on the latitude as well as on the altitude), the thermodynamics of the ice sheet including sliding and the bedrock uplift (using a constant relaxation time). They have found thermodynamics to be necessary for the appearance of oscillations. Even though the amplitude and period found by Oerlemans (1982) are very sensitive to parameter choice, the free oscillations seem to be a robust feature of that model over a wide range of parameter values, confirming that the interaction of both feedback shown in Fig. 1 can indeed generate robust oscillation.

In order to make sure that the observed dynamical regimes discussed in the present study, in particular the oscillating regime, are not an artifact produced by specific modeling choices, we perform several robustness checks. In the following the impact of some assumptions made for the bedrock model and for the climatic mass balance is tested for one set of parameters ($\Gamma = 6$ K/km, $\Delta T = 2$ K, $\eta = 1 \times 10^{21}$ Pa$\cdot$s.).

Changing the bedrock uplift model to the instantaneous point-wise isostacy model, defined as

$$b(t,x,y) = b(0,x,y) - \frac{\rho_i}{\rho_m}\left[H(t,x,y) - H(0,x,y)\right],$$

and leaving all other parameters and modeling choices fixed produces very similar oscillations to the reference run (see Fig. 8). Recovering an oscillating regime with instantaneous isostacy shows that the time lag between ice load change and full uplift is not the only driver of the oscillation. The change in bedrock model causes a decrease in amplitude, by shifting the minimal volume up, and an increase in oscillation time.

Including the precipitation scaling of 7.3% per degree Celsius of global mean temperature change, in contrast to the fixed precipitation field, mitigates the ice losses and leads to higher minimal and maximal volumes and a decrease in oscillation amplitude and an increase in oscillation time.

In order to test the impact of the initial state, a different spin-up was performed in addition to the equilibrium spin-up, which was used for the standard runs. Here we use a spin-up similar to the "paleo-climate spin-up" in Aschwanden et al. (2013) over the last 125 kyrs. However, the simulation of the past 125 kyrs including bedrock deformation is performed twice, adding the anomaly of the bedrock topography at the end of the first run to the initial state of the second run. Therefore an initial state closer to present day topography is obtained at the end of the second run, and the bedrock is in equilibrium with the ice topography. Using this paleo-climate spin up with explicit treatment of the bedrock still recovers the oscillatory regime for the first 300 kyrs (see Fig. 8 c). In contrast to the reference run, the amplitude of the oscillation decreases with time and a stable plateau is observed in the past 150 kyrs.

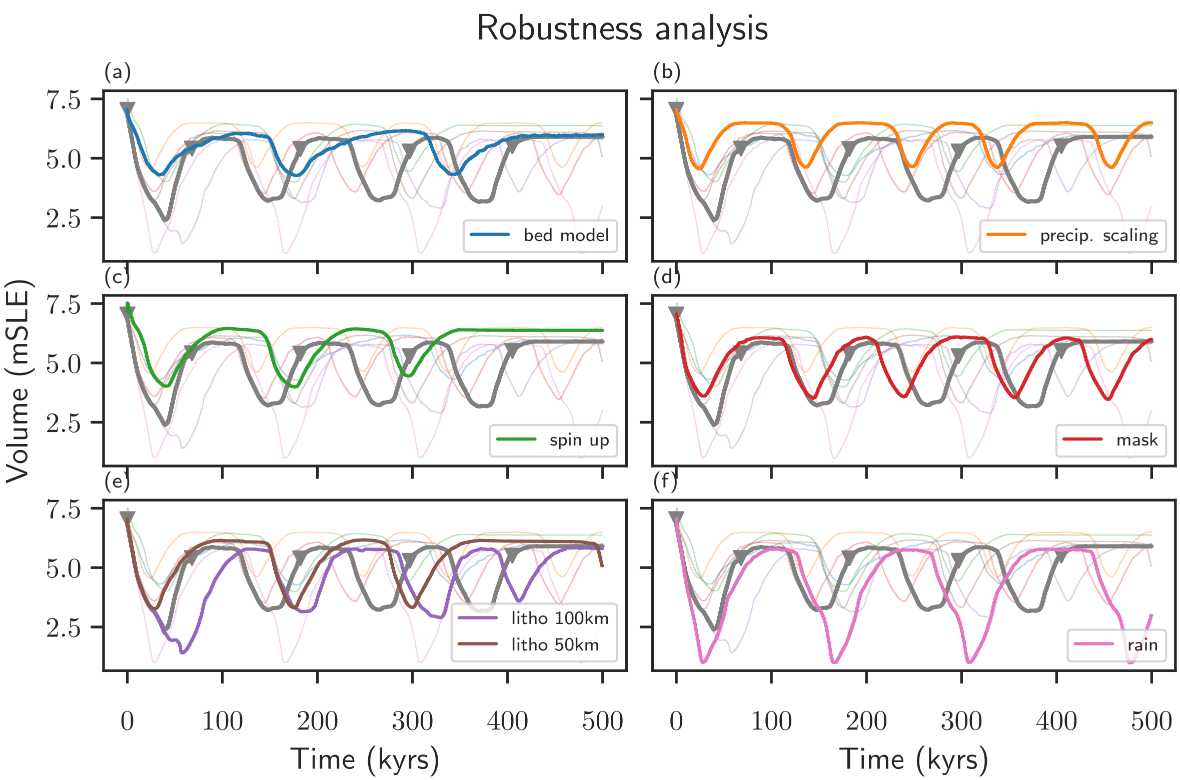

Figure 8. Robustness analysis for the simulation run with parameters $\Gamma = 6$ K/km, $\Delta T = 2$ K, $\eta = 1 \times 10^{21}$ Pa·s. The gray curve corresponds to the reference run, also shown in Fig. 2 and 3 and is shown in each panel for reference. The colored faint lines provide context. Each change in modeling choice is highlighted in its own panel. (a) Run with a intantaneous pointwise isostacy model. (b) Run which includes a 7.3% precipitation increase per degree Celsius of global mean temperature increase. (c) Run which starts from a glacial spin-up. (d) Run which omits the flux correction at the ice-free margin. (e) Runs with two different lithosphere thicknesses, 100 km and 50 km. (f) Run, which uses a different interpolation between rain and snow.

In the reference run we adapted the climatic mass balance in the areas which are ice-free under present day in order to keep them ice-free, such that the initial state would not grow beyond the area of present day ice sheet. The flux correction at the ice free margins has only a minor effect on the oscillating regime (see Fig. 8). The oscillation amplitude is barely altered, the oscillation time is slightly shorter, and the initial ice loss is less deep compared to the reference run. However, the volume of the unforced control run grows from 7.06 m to 7.62 m.

The influence of the lithosphere thickness, which can be altered indirectly through a different flexural rigidity of the lithosphere, which is proportional to the third power of the lithosphere thickness. Increasing the lithosphere thickness from 88 km to 100 km increases the initial ice loss and the oscillation time, however the long-term amplitude of the oscillation and the minimal and maximal volume remain almost unaffected. Decreasing the lithosphere thickness to 50 km reduces the initial ice loss and increases the maximal volume of the oscillation. An almost stable plateau of approx. 150 kyrs appears after 350 kyrs of simulation time, but a dip in the ice volume is observed at the end of the oscillation time, indicating that the plateau is not stable on the long term.

In the reference run all precipitation is perceived as snow if the local mean temperature is below 0°C and all precipitation is perceived as rain if the local mean temperature is above 2°C, with a linear interpolation in between. Changing the critical temperatures to -1°C and 3°C allows a bigger window where both, rain and snow are present. This change introduces a larger oscillation amplitude and reduces the oscillation time (see Fig. 8 f).

The modeling choices will most likely also affect the distribution of the dynamical regimes in the parameter landscape as shown in Fig. 4, and changing more than one modeling choice at one would introduce stronger changes. For instance changing the spin-up and flux correction (see Fig. 8, c and d) at once shifts the regime from "oscillation" to "incomplete recovery". Recreating simulations for the full parameter space for each of the modeling choices and different combinations of those is, unfortunately, beyond the scope of this paper. However, we have shown that the oscillating regimes of the Greenland Ice Sheet under constant temperature forcing are robust against many modeling choices and is unlikely to be an artifact created by one particular simulation setup.

4.4 Limitations

This study is based on the results of the ice sheet model PISM coupled to simple models which capture the melt-elevation feedback, namely the positive degree day approach together with an atmospheric temperature lapse rate, and the GIA feedback, namely the Lingle-Clark model. The relative computational efficiency of those models allows us to conduct an ensemble of long-term simulations over 500,000 years exploring different parameter values characterizing the individual feedbacks and warming. This approach fits the conceptual research question of this study.

The Lingle-Clark approach assumes a flat earth with two layers, one elastic and one viscous layer, in contrast to more sophisticated solid Earth models. It also does assume horizontally constant Earth structure and does not solve the self-consistent sea-level equation. However, the relative importance of discharge and melt at the ice-ocean interface decreases with ongoing warming, as the tidewater glaciers retreat and the ice-ocean interface shrinks ~~(?)~~(Aschwanden et al., 2019). With ongoing coupling efforts between ice-dynamics models and process based solid Earth models, this study is a first step to assessing the importance of the GIA feedback for the stability of the Greenland Ice Sheet.

While the design of the study was chosen in order to allow for long experiments and to cover parts of the parameter space (ΔT, Γ, and $\cancel{\nu}\eta$), it is also one of the main limitations of the study. The coarse resolution of the ice sheet model does not adequately resolve the flow patterns in outlet glaciers, therefore underestimating dynamical ice losses. Moreover, the parameters which govern the ice dynamics, although uncertain, were not varied (Zeitz et al., 2020).

The choice of the positive degree day (PDD) method in order to compute the climatic mass balance introduces a tends to underestimate the melt area for present climate, while at high temperatures PDD tends to overestimate melt. Moreover, the temperature anomaly is applied in a spatially and temporally constant way and the precipitation pattern remains fixed~~.~~, without any adaption to the temperature forcing. A more realistic approach would include the increase of precipitation with warmer air temperature and partially mitigate ice losses. However in this rather conceptual study we explore the stability landscape without taking the increase in precipitation into account, as it reduces the complexity of the system. We have shown in 4.3 that while the total ice losses are reduced when considering the increase in precipitation, the qualitative dynamics remains the same (oscillations). So far, scenario-based projections of future global warming are limited until the year 2300, with projections of the temperature evolution and changes in climatic mass balance over the Greenland Ice Sheet as results from regional climate models only available until the end of this century. The aim here, however, is not to present scenario-based projections of future ice losses but rather to study the distinct dynamical states in the "deep future" of the Greenland Ice Sheet in a fundamental way.

5 Conclusions

Here we present an analysis of the dynamic regimes in the deep future of the Greenland Ice Sheet. Depending on the amount of warming and the values of the parameters describing the strength of the melt-elevation feedback and the GIA feedback we find that four different dynamic regimes can be realized: 1) Direct stabilization into a new equilibrium state which preserves 90% or more of the initial ice volume, 2) ~~Recovery~~ Incomplete recovery to a stable state after an initial ice loss, 3) Self-sustained oscillations, and 4) Irreversible loss of a large portion of the ice. Our model configuration with parameterized melt-elevation feedback and a fast computation of the leading-order GIA effects allows for studying an ensemble of glacial time-scale simulations and provides insight into how the interaction of feedbacks impacts the dynamics of the complex Earth system with implications for Earth system stability and resilience. Although it is not explicitly studied here, drastic changes in the ice volume of the Greenland Ice Sheet would have implications for the global earth system via global sea level rise, changes in the planetary albedo, and changes in the atmospheric and oceanic circulation patterns as the Jetstream or the Atlantic Meridional Overturning Circulation (AMOC).

Code availability. The PISM source code is freely available.

Appendix A: Relaxation times in the Lingle-Clark model

Following Bueler et al. (2007), Eq. (14), the relaxation time of the Lingle-Clark model can be computed as a function of the load change wavelength λ from comparison to the ELRA model as

$$\tau(\lambda) = \frac{4\pi\eta|\lambda|^{-1}}{\rho_m g + 16\pi^4 D\lambda^{-4}}.$$

As the relaxation time is directly proportional to the mantle viscosity η the maximal relaxation time increases by more than two orders of magnitude over the tested parameter range. The changes in lithosphere thickness induce less changes to the relaxation time spectrum. Wavelengths relevant for the deglaciation of the Greenland Ice Sheet are between several tens of kilometers (onset of retreat) to 500-1500 km (the spatial extent of the Greenland Ice Sheet).

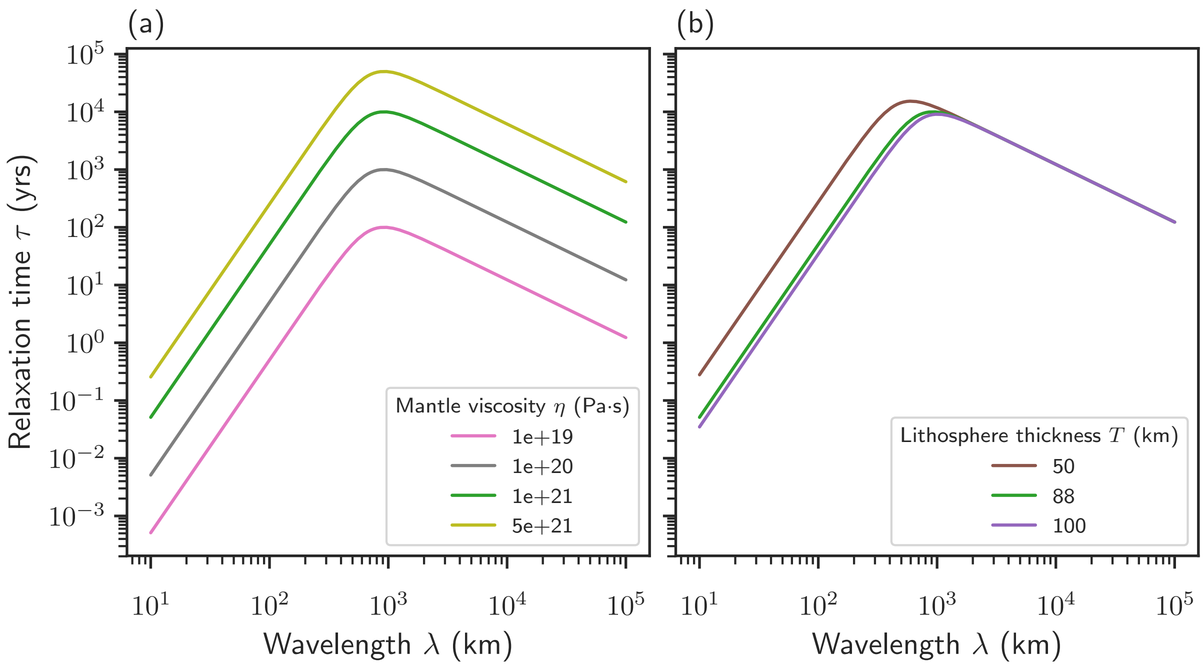

Figure A1. Spectrum of the relaxation time vs. wavelength of the load change for different mantle viscosities and lithosphere thicknesses, as shown in Bueler et al. (2007), Eq. (14)

Author contributions. RW conceived this study. JH prepared and analysed the initial experiments during his Master project, advised by RW and MZ. MZ expanded the experiments, visualized the results and wrote the manuscript, with support from RW and JFD and TA. All authors interpreted and discussed the results. All the authors give their final approval of the article version to be published.

Competing interests. The authors declare no competing interests.

Acknowledgements. We would like to thank Anders Levermann and Fuyuki Saito for fruitful discussion. We are grateful for financial support by the European Research Council Advanced Grant project ERA (Earth Resilience in the Anthropocene, grant ERC-2016-ADG-743080) and the Leibniz Association (project DominoES). MZ is partially supported by the Deutsche Forschungsgemeinschaft (DFG) by grant WI4556/3-1. MZ acknowledges the German Fulbright commission for a PhD program. RW and TA acknowledge support by TiPACCs, PROTECT, PalMod. We further acknowledge the European Regional Development Fund (ERDF), the German Federal Ministry of Education and Research (BMBF) and the Land Brandenburg for supporting this project by providing resources on the high-performance computer system at the Potsdam Institute for Climate Impact Research. Development of PISM is supported by NASA grant NNX17AG65G and NSF grants PLR-1603799 and PLR-1644277.

References

Abe-Ouchi, A., Saito, F., Kawamura, K., Raymo, M. E., Okuno, J., Takahashi, K., and Blatter, H.: Insolation-driven 100,000-year glacial cycles and hysteresis of ice-sheet volume, Nature, 500, 190–193, https://doi.org/10.1038/nature12374, 2013.

Adhikari, S., Ivins, E. R., and Larour, E. Y.: Mass transport waves amplified by intense Greenland melt and detected in solid Earth deformation, Geophysical Research Letters, 44, 4965–4975, https://doi.org/10.1002/2017GL073478, 2017.

Adhikari, S., Milne, G. A., Caron, L., Khan, S. A., Kjeldsen, K. K., Nilsson, J., Larour, E. Y., and Ivins, E. R.: Decadal to Centennial Timescale Mantle Viscosity Inferred From Modern Crustal Uplift Rates in Greenland, Geophysical Research Letters, 48, 1–11, https://doi.org/10.1029/2021gl094040, 2021.

Albrecht, T., Winkelmann, R., and Levermann, A.: Glacial-cycle simulations of the Antarctic Ice Sheet with the Parallel Ice Sheet Model (PISM) – Part 1: Boundary conditions and climatic forcing, The Cryosphere, 14, 599–632, https://doi.org/10.5194/tc-14-599-2020, https://tc.copernicus.org/articles/14/599/2020/, 2020.

Alkhayuon, H., Ashwin, P., Jackson, L. C., Quinn, C., and Wood, R. A.: Basin bifurcations, oscillatory instability and rate-induced thresholds for Atlantic meridional overturning circulation in a global oceanic box model, Proceedings of the Royal Society A: Mathematical, Physical and Engineering Sciences, 475, https://doi.org/10.1098/rspa.2019.0051, 2019.

Aschwanden, A., Aðalgeirsdóttir, G., and Khroulev, C.: Hindcasting to measure ice sheet model sensitivity to initial states, The Cryosphere, 7, 1083–1093, https://doi.org/10.5194/tc-7-1083-2013, https://tc.copernicus.org/articles/7/1083/2013/, 2013.

Aschwanden, A., Fahnestock, M. A., and Truffer, M.: Complex Greenland outlet glacier flow captured, Nature Communications, 7, 10 524, https://doi.org/10.1038/ncomms10524, http://dx.doi.org/10.1038/ncomms10524, 2016.

Aschwanden, A., Fahnestock, M. A., Truffer, M., Brinkerhoff, D. J., Hock, R., Khroulev, C., Mottram, R. H., and Khan, S. A.: Contribution of the Greenland Ice Sheet to sea level over the next millennium, Science Advances, 5, eaav9396, https://doi.org/10.1126/sciadv.aav9396, http://advances.sciencemag.org/lookup/doi/10.1126/sciadv.aav9396, 2019.

Barletta, V. R., Bevis, M., Smith, B. E., Wilson, T., Brown, A., Bordoni, A., Willis, M. J., Khan, S. A., Rovira-Navarro, M., Dalziel, I., Smalley, R., Kendrick, E., Konfal, S., Caccamise, D. J., Aster, R. C., Nyblade, A., and Wiens, D. A.: Observed rapid bedrock uplift in amundsen sea embayment promotes ice-sheet stability, Science, 360, 1335–1339, https://doi.org/10.1126/science.aao1447, 2018.

Bassis, J. N., Petersen, S. V., and Mac Cathles, L.: Heinrich events triggered by ocean forcing and modulated by isostatic adjustment, Nature, 542, 332–334, https://doi.org/10.1038/nature21069, 2017.

Boers, N. and Rypdal, M.: Critical slowing down suggests that the western Greenland Ice Sheet is close to a tipping point, Proceedings of the National Academy of Sciences of the United States of America, 118, 1–7, https://doi.org/10.1073/pnas.2024192118, 2021.

Braithwaite, R. J.: Positive degree-day factors for ablation on the Greenland ice sheet studied by energy-balance modelling, Journal of Glaciology, 41, 153–160, https://doi.org/10.1017/S0022143000017846, 1995.

Bueler, E. and Brown, J.: Shallow shelf approximation as a "sliding law" in a thermomechanically coupled ice sheet model, Journal of Geophysical Research: Solid Earth, 114, 1–21, https://doi.org/10.1029/2008JF001179, 2009.

Bueler, E. and van Pelt, W.: Mass-conserving subglacial hydrology in the Parallel Ice Sheet Model version 0.6, Geoscientific Model Development, 8, 1613–1635, https://doi.org/10.5194/gmd-8-1613-2015, https://gmd.copernicus.org/articles/8/1613/2015/, 2015.

Bueler, E., Lingle, C. S., and Brown, J.: Fast computation of a viscoelastic deformable Earth model for ice-sheet simulations, Annals of Glaciology, 46, 97–105, https://doi.org/10.3189/172756407782871567, 2007.

Crucifix, M.: Oscillators and relaxation phenomena in Pleistocene climate theory, Philosophical Transactions of the Royal Society A: Mathematical, Physical and Engineering Sciences, 370, 1140–1165, https://doi.org/10.1098/rsta.2011.0315, 2012.

De Boer, B., Stocchi, P., and van de Wal, R. S. W.: A fully coupled 3-D ice-sheet-sea-level model: Algorithm and applications, Geoscientific Model Development, 7, 2141–2156, https://doi.org/10.5194/gmd-7-2141-2014, 2014.

Denton, G. H., Anderson, R. F., Toggweiler, J. R., Edwards, R. L., Schaefer, J. M., and Putnam, A. E.: The Last Glacial Termination, Science, 328, 1652–1656, https://doi.org/10.1126/science.1184119, 2010.

Dietrich, R., Rülke, A., and Scheinert, M.: Present-day vertical crustal deformations in West Greenland from repeated GPS observations, Geophysical Journal International, 163, 865–874, https://doi.org/10.1111/j.1365-246X.2005.02766.x, 2005.

Farrell, W. E. and Clark, J. A.: On Postglacial Sea Level, Geophysical Journal of the Royal Astronomical Society, 46, 647–667, https://doi.org/10.1111/j.1365-246X.1976.tb01252.x, 1976.

Fausto, R. S., Ahlstrøm, A. P., Van As, D., Bøggild, C. E., and Johnsen, S. J.: A new present-day temperature parameterization for Greenland, Journal of Glaciology, 55, 95–105, https://doi.org/10.3189/002214309788608985, https://www.cambridge.org/core/product/identifier/S0022143000200099/type/journal{_}article, 2009.

Feldmann, J. and Levermann, A.: From cyclic ice streaming to Heinrich-like events: the grow-and-surge instability in the Parallel Ice Sheet Model, The Cryosphere, 11, 1913–1932, https://doi.org/10.5194/tc-11-1913-2017, https://tc.copernicus.org/articles/11/1913/2017/, 2017.

Fettweis, X., Hofer, S., Krebs-Kanzow, U., Amory, C., Aoki, T., Berends, C. J., Born, A., Box, J. E., Delhasse, A., Fujita, K., Gierz, P., Goelzer, H., Hanna, E., Hashimoto, A., Huybrechts, P., Kapsch, M.-l., King, M. D., Kittel, C., Lang, C., Langen, P. L., Lenaerts, J. T. M., Liston, G. E., Lohmann, G., Mernild, S. H., Mikolajewicz, U., Modali, K., Mottram, R. H., Niwano, M., Noël, B., Ryan, J. C., Smith, A., Streffing, J., Tedesco, M., van de Berg, W. J., van den Broeke, M., van de Wal, R. S. W., van Kampenhout, L., Wilton, D. J., Wouters, B., Ziemen, F., and Zolles, T.: GrSMBMIP: intercomparison of the modelled 1980–2012 surface mass balance over the Greenland Ice Sheet, The Cryosphere, 14, 3935–3958, https://doi.org/10.5194/tc-14-3935-2020, https://tc.copernicus.org/articles/14/3935/2020/, 2020.

Fleming, K. and Lambeck, K.: Constraints on the Greenland Ice Sheet since the Last Glacial Maximum from sea-level observations and glacial-rebound models, Quaternary Science Reviews, 23, 1053–1077, https://doi.org/10.1016/j.quascirev.2003.11.001, 2004.

Frederikse, T., Landerer, F. W., Caron, L., Adhikari, S., Parkes, D., Humphrey, V. W., Dangendorf, S., Hogarth, P., Zanna, L., Cheng, L., and Wu, Y. H.: The causes of sea-level rise since 1900, Nature, 584, 393–397, https://doi.org/10.1038/s41586-020-2591-3, http://dx.doi.org/10.1038/s41586-020-2591-3, 2020.

Ganopolski, A. and Calov, R.: The role of orbital forcing, carbon dioxide and regolith in 100 kyr glacial cycles, Climate of the Past, 7, 1415–1425, https://doi.org/10.5194/cp-7-1415-2011, 2011.

Gardner, A. S., Sharp, M. J., Koerner, R. M., Labine, C., Boon, S., Marshall, S. J., Burgess, D. O., and Lewis, D.: Near-surface temperature lapse rates over arctic glaciers and their implications for temperature downscaling, Journal of Climate, 22, 4281–4298, https://doi.org/10.1175/2009JCLI2845.1, 2009.

Ghil, M. and Lucarini, V.: The physics of climate variability and climate change, Reviews of Modern Physics, 92, 35 002, https://doi.org/10.1103/RevModPhys.92.035002, https://doi.org/10.1103/RevModPhys.92.035002, 2020.

Gomez, N., Pollard, D., and Mitrovica, J. X.: A 3-D coupled ice sheet - sea level model applied to Antarctica through the last 40 ky, Earth and Planetary Science Letters, 384, 88–99, https://doi.org/10.1016/j.epsl.2013.09.042, http://dx.doi.org/10.1016/j.epsl.2013.09.042, 2013.

Gomez, N., Latychev, K., and Pollard, D.: A coupled ice sheet-sea level model incorporating 3D earth structure: Variations in Antarctica during the Last Deglacial Retreat, Journal of Climate, 31, 4041–4054, https://doi.org/10.1175/JCLI-D-17-0352.1, 2018.

Gomez, N., Weber, M. E., Clark, P. U., Mitrovica, J. X., and Han, H. K.: Antarctic ice dynamics amplified by Northern Hemisphere sea-level forcing, Nature, 587, 600–604, https://doi.org/10.1038/s41586-020-2916-2, http://dx.doi.org/10.1038/s41586-020-2916-2, 2020.

Haeger, C., Kaban, M. K., Tesauro, M., Petrunin, A. G., and Mooney, W. D.: 3-D Density, Thermal, and Compositional Model of the Antarctic Lithosphere and Implications for Its Evolution, Geochemistry, Geophysics, Geosystems, 20, 688–707, https://doi.org/10.1029/2018GC008033, 2019.

Hagedoorn, J. M., Wolf, D., and Martinec, Z.: An estimate of global mean sea-level rise inferred from tide-gauge measurements using glacial-isostatic models consistent with the relative sea-level record, Pure and Applied Geophysics, 164, 791–818, https://doi.org/10.1007/s00024-007-0186-7, 2007.

Hanna, E., Huybrechts, P., Janssens, I., Cappelen, J., Steffen, K., and Stenhens, A.: Runoff and mass balance of the Greenland ice sheet: 1958-2003, Journal of Geophysical Research Atmospheres, 110, 1–16, https://doi.org/10.1029/2004JD005641, 2005.

IMBIE Team: Mass balance of the Greenland Ice Sheet from 1992 to 2018., Nature, 579, 233–239, https://doi.org/10.1038/s41586-019-1855-2, http://www.nature.com/articles/s41586-019-1855-2http://www.ncbi.nlm.nih.gov/pubmed/31822019, 2020.

Joughin, I., Smith, B. E., and Howat, I. M.: Greenland Ice Mapping Project: ice flow velocity variation at sub-monthly to decadal timescales, The Cryosphere, 12, 2211–2227, https://doi.org/10.5194/tc-12-2211-2018, https://tc.copernicus.org/articles/12/2211/2018/, 2018.

Khan, S. A., Wahr, J., Leuliette, E., van Dam, T., Larson, K. M., and Francis, O.: Geodetic measurements of postglacial adjustments in Greenland, Journal of Geophysical Research: Solid Earth, 113, 1–16, https://doi.org/10.1029/2007JB004956, 2008.

Khan, S. A., Sasgen, I., Bevis, M., van Dam, T., Bamber, J. L., Wahr, J., Willis, M. J., Kjær, K. H., Wouters, B., Helm, V., Csatho, B., Fleming, K., Bjørk, A. A., Aschwanden, A., Knudsen, P., and Munneke, P. K.: Geodetic measurements reveal similarities between post–Last Glacial Maximum and present-day mass loss from the Greenland ice sheet, Science Advances, 2, e1600 931, https://doi.org/10.1126/sciadv.1600931, http://advances.sciencemag.org.biblioplanets.gate.inist.fr/content/2/9/e1600931, 2016.

Khroulev, C. and the PISM authors: PISM, a Parallel Ice Sheet Model v2.0: User's Manual, https://www.pism.io/docs/manual/, 2021.

Kingslake, J., Scherer, R. P., Albrecht, T., Coenen, J., Powell, R. D., Reese, R., Stansell, N. D., Tulaczyk, S., Wearing, M. G., and Whitehouse, P. L.: Extensive retreat and re-advance of the West Antarctic Ice Sheet during the Holocene, Nature, 558, 430–434, https://doi.org/10.1038/s41586-018-0208-x, http://dx.doi.org/10.1038/s41586-018-0208-xhttp://www.nature.com/articles/s41586-018-0208-x, 2018.

Konrad, H., Sasgen, I., Pollard, D., and Klemann, V.: Potential of the solid-Earth response for limiting long-term West Antarctic Ice Sheet retreat in a warming climate, Earth and Planetary Science Letters, 432, 254–264, https://doi.org/10.1016/j.epsl.2015.10.008, http://dx.doi.org/10.1016/j.epsl.2015.10.008, 2015.

Lambeck, K., Rouby, H., Purcell, A., Sun, Y., and Sambridge, M.: Sea level and global ice volumes from the Last Glacial Maximum to the Holocene, Proceedings of the National Academy of Sciences of the United States of America, 111, 15 296–15 303, https://doi.org/10.1073/pnas.1411762111, 2014.

Larour, E. Y., Seroussi, H., Adhikari, S., Ivins, E. R., Caron, L., Morlighem, M., and Schlegel, N.: Slowdown in Antarctic mass loss from solid Earth and sea-level feedbacks, Science, 364, eaav7908, https://doi.org/10.1126/science.aav7908, https://www.sciencemag.org/lookup/doi/10.1126/science.aav7908, 2019.

Lau, H. C., Mitrovica, J. X., Austermann, J., Crawford, O., Al-Attar, D., and Latychev, K.: Inferences of mantle viscosity based on ice age data sets: Radial structure, Journal of Geophysical Research: Solid Earth, 121, 6991–7012, https://doi.org/10.1002/2016JB013043, 2016.

Le Meur, E. and Huybrechts, P.: A comparison of different ways of dealing with isostasy: examples from modelling the Antarctic ice sheet during the last glacial cycle, Annals of Glaciology, 23, 309–317, https://doi.org/10.1017/S0260305500013586, https://www.cambridge.org/core/product/identifier/S0260305500013586/type/journal{_}article, 1996.

Le Meur, E. and Huybrechts, P.: Present-day uplift patterns over Greenland from a coupled ice-sheet/visco-elastic bedrock model, Geophysical Research Letters, 25, 3951–3954, https://doi.org/10.1029/1998GL900052, 1998.

Le Meur, E. and Huybrechts, P.: A model computation of the temporal changes of surface gravity and geoidal signal induced by the evolving greenland ice sheet, Geophysical Journal International, 145, 835–849, https://doi.org/10.1046/j.1365-246X.2001.01442.x, 2001.

Lecavalier, B. S., Milne, G. A., Simpson, M. J., Wake, L. M., Huybrechts, P., Tarasov, L., Kjeldsen, K. K., Funder, S., Long, A. J., Woodroffe, S., Dyke, A. S., and Larsen, N. K.: A model of Greenland ice sheet deglaciation constrained by observations of relative sea level and ice extent, Quaternary Science Reviews, 102, 54–84, https://doi.org/10.1016/j.quascirev.2014.07.018, http://dx.doi.org/10.1016/j.quascirev.2014.07.018, 2014.

Lenton, T. M., Rockström, J., Gaffney, O., Rahmstorf, S., Richardson, K., Steffen, W., and Shellnhuber, H. J.: Climate tipping points - too risky to bet against, Nature, 575, 592–595, 2019.

Levermann, A. and Winkelmann, R.: A simple equation for the melt elevation feedback of ice sheets, The Cryosphere, 10, 1799–1807, https://doi.org/10.5194/tc-10-1799-2016, https://tc.copernicus.org/articles/10/1799/2016/, 2016.

Levermann, A., Albrecht, T., Winkelmann, R., Martin, M. A., Haseloff, M., and Joughin, I.: Kinematic first-order calving law implies potential for abrupt ice-shelf retreat, The Cryosphere, 6, 273–286, https://doi.org/10.5194/tc-6-273-2012, https://tc.copernicus.org/articles/6/273/2012/, 2012.

Levermann, A., Clark, P. U., Marzeion, B., Milne, G. A., Pollard, D., Radic, V., and Robinson, A.: The multimillennial sea-level commitment of global warming., Proceedings of the National Academy of Sciences, 110, 13 745–13 750, https://doi.org/10.1073/pnas.1219414110, http://www.ncbi.nlm.nih.gov/pubmed/23858443, 2013.

Lingle, C. S. and Clark, J. A.: A numerical model of interactions between a marine ice sheet and the solid Earth: application to a West Antarctic ice stream., Journal of Geophysical Research, 90, 1100–1114, https://doi.org/10.1029/JC090iC01p01100, 1985.

Locarnini, R. A., Mishonov, A., Baranova, O., Boyer, T. P., Zweng, M., Garcia, H. E., Reagan, J., Seidov, D., Weathers, K. W., Paver, C., and Smolyar, I. V.: WORLD OCEAN ATLAS 2018 Volume 1: Temperature, Tech. rep., 2019.

Ma, Y., Gagliardini, O., Ritz, C., Gillet-Chaulet, F., Durand, G., and Montagnat, M.: Enhancement factors for grounded ice and ice shelves inferred from an anisotropic ice-flow model, Journal of Glaciology, 56, 805–812, https://doi.org/10.3189/002214310794457209, http://www.agu.org/pubs/crossref/2011/2011GL048892.shtmlhttps://www.cambridge.org/core/product/identifier/S0022143000214068/type/journal{_}article, 2010.

Martinec, Z.: Spectral-finite element approach to three-dimensional viscoelastic relaxation in a spherical earth, Geophysical Journal International, 142, 117–141, https://doi.org/10.1046/j.1365-246X.2000.00138.x, 2000.

Milne, G. A., Latychev, K., Schaeffer, A., Crowley, J. W., Lecavalier, B. S., and Audette, A.: The influence of lateral Earth structure on glacial isostatic adjustment in Greenland, Geophysical Journal International, 214, 1252–1266, https://doi.org/10.1093/GJI/GGY189, 2018.

Mordret, A.: Uncovering the Iceland Hot Spot Track Beneath Greenland, Journal of Geophysical Research: Solid Earth, 123, 4922–4941, https://doi.org/10.1029/2017JB015104, 2018.

Morlighem, M., Bondzio, J., Seroussi, H., Rignot, E., Larour, E. Y., Humbert, A., and Rebuffi, S.: Modeling of Store Gletscher's calving dynamics, West Greenland, in response to ocean thermal forcing, Geophysical Research Letters, 43, 2659–2666, https://doi.org/10.1002/2016GL067695, 2016.

Morlighem, M., Williams, C. N., Rignot, E., An, L., Arndt, J. E., Bamber, J. L., Catania, G., Chauché, N., Dowdeswell, J. A., Dorschel, B., Fenty, I. G., Hogan, K., Howat, I. M., Hubbard, A., Jakobsson, M., Jordan, T. M., Kjeldsen, K. K., Millan, R., Mayer, L., Mouginot, J., Noël, B. P. Y., O'Cofaigh, C., Palmer, S., Rysgaard, S., Seroussi, H., Siegert, M. J., Slabon, P., Straneo, F., van den Broeke, M. R., Weinrebe, W., Wood, M., and Zinglersen, K. B.: BedMachine v3: Complete Bed Topography and Ocean Bathymetry Mapping of Greenland From Multibeam Echo Sounding Combined With Mass Conservation, Geophysical Research Letters, 44, 11,051–11,061, https://doi.org/10.1002/2017GL074954, 2017.

Mouginot, J., Rignot, E., Bjørk, A. A., Van Den Broeke, M. R., Millan, R., Morlighem, M., Noël, B. P. Y., Scheuchl, B., and Wood, M.: Forty-six years of Greenland Ice Sheet mass balance from 1972 to 2018, Proceedings of the National Academy of Sciences, 116, 201904 242, https://doi.org/10.1073/pnas.1904242116, http://www.pnas.org/lookup/doi/10.1073/pnas.1904242116, 2019.

Noël, B. P. Y., van de Berg, W. J., Lhermitte, S., and van den Broeke, M. R.: Rapid ablation zone expansion amplifies north Greenland mass loss, Science Advances, 5, 2–11, https://doi.org/10.1126/sciadv.aaw0123, 2019.

Oerlemans, J.: Glacial cycles and ice-sheet modelling, Climatic Change, 4, 353–374, https://doi.org/10.1007/BF02423468, http://link.springer.com/10.1007/BF02423468, 1982.

Peltier, W. R. and Drummong, R.: Rheological stratification of the lithosphere: A direct inference based upon the geodetically observed pattern of the glacial isostatic adjustment of the North American continent, Geophysical Research Letters, 35, 1–5, https://doi.org/10.1029/2008GL034586, 2008.

Petrini, M., Vizcaíno, M., Sellevold, R., Muntjewerf, L., Georgiou, S., Scherrenberg, M. D. W., Lipscomb, W., and Leguy, G. R.: Multi-millennial response of the Greenland Ice Sheet to anthropogenic warming, in: EGU General Assembly 2021, online, 19–30 Apr 2021, EGU21-12958, https://doi.org/doi.org/10.5194/egusphere-egu21-12958, 2021.

Pico, T., Birch, L., Weisenberg, J., and Mitrovica, J. X.: Refining the Laurentide Ice Sheet at Marine Isotope Stage 3: A data-based approach combining glacial isostatic simulations with a dynamic ice model, Quaternary Science Reviews, 195, 171–179, https://doi.org/10.1016/j.quascirev.2018.07.023, https://doi.org/10.1016/j.quascirev.2018.07.023, 2018.

Pollard, D., Gomez, N., and Deconto, R. M.: Variations of the Antarctic Ice Sheet in a Coupled Ice Sheet-Earth-Sea Level Model: Sensitivity to Viscoelastic Earth Properties, Journal of Geophysical Research: Earth Surface, 122, 2124–2138, https://doi.org/10.1002/2017JF004371, 2017.

Powell, E. M., Gomez, N., Hay, C., Latychev, K., and Mitrovica, J. X.: Viscous effects in the solid earth response to modern Antarctic ice mass flux: Implications for geodetic studies of WAIS stability in a warming world, Journal of Climate, 33, 443–459, https://doi.org/10.1175/JCLI-D-19-0479.1, 2020.

Powell, E. M., Pan, L., Hoggard, M. J., Latychev, K., Gomez, N., Austermann, J., and Mitrovica, J. X.: The impact of 3-D Earth structure on far-field sea level following interglacial West Antarctic Ice Sheet collapse, Quaternary Science Reviews, 273, 107 256, https://doi.org/10.1016/j.quascirev.2021.107256, https://doi.org/10.1016/j.quascirev.2021.107256, 2021.

Rignot, E. and Mouginot, J.: Ice flow in Greenland for the International Polar Year 2008-2009, Geophysical Research Letters, 39, 1–7, https://doi.org/10.1029/2012GL051634, 2012.

Robinson, A., Calov, R., and Ganopolski, A.: Multistability and critical thresholds of the Greenland ice sheet, Nature Climate Change, 2, 429–432, https://doi.org/10.1038/nclimate1449, http://dx.doi.org/10.1038/nclimate1449, 2012.

Schumacher, M., King, M. A., Rougier, J., Sha, Z., Khan, S. A., and Bamber, J. L.: A new global GPS data set for testing and improving modelled GIA uplift rates, Geophysical Journal International, 214, 2164–2176, https://doi.org/10.1093/gji/ggy235, 2018.

Simpson, M. J., Milne, G. A., Huybrechts, P., and Long, A. J.: Calibrating a glaciological model of the Greenland ice sheet from the Last Glacial Maximum to present-day using field observations of relative sea level and ice extent, Quaternary Science Reviews, 28, 1631–1657, https://doi.org/10.1016/j.quascirev.2009.03.004, http://dx.doi.org/10.1016/j.quascirev.2009.03.004, 2009.

Steffen, K. and Box, J. E.: Surface climatology of the Greenland Ice Sheet: Greenland Climate Network 1995-1999, Journal of Geophysical Research: Atmospheres, 106, 33 951–33 964, https://doi.org/10.1029/2001JD900161, http://doi.wiley.com/10.1029/2001JD900161, 2001.

Talento, S. and Ganopolski, A.: Reduced-complexity model for the impact of anthropogenic CO2 emissions on future glacial cycles, Earth System Dynamics, 12, 1275–1293, https://doi.org/10.5194/esd-12-1275-2021, https://esd.copernicus.org/articles/12/1275/2021/, 2021.

the PISM authors: PISM, a Parallel Ice Sheet Model, http://www.pism-docs.org, 2018.

Tosi, N., Sabadini, R., Marotta, A. M., and Vermeersen, L. L.: Simultaneous inversion for the Earth's mantle viscosity and ice mass imbalance in Antarctica and Greenland, Journal of Geophysical Research: Solid Earth, 110, 1–14, https://doi.org/10.1029/2004JB003236, 2005.

Vasskog, K., Langebroek, P. M., Andrews, J. T., Nilsen, J. E. Ø., and Nesje, A.: The Greenland Ice Sheet during the last glacial cycle: Current ice loss and contribution to sea-level rise from a palaeoclimatic perspective, Earth-Science Reviews, 150, 45–67, https://doi.org/10.1016/j.earscirev.2015.07.006, http://dx.doi.org/10.1016/j.earscirev.2015.07.006, 2015.

Wahr, J., van Dam, T., Larson, K. M., and Francis, O.: Geodetic measurements in Greenland and their implications, Journal of Geophysical Research: Solid Earth, 106, 16 567–16 581, https://doi.org/10.1029/2001JB000211, http://doi.wiley.com/10.1029/2001JB000211, 2001.

Weertman, J.: Stability of ice-age ice sheets, Journal of Geophysical Research, 66, 3783–3792, https://doi.org/10.1029/jz066i011p03783, 1961.

Whitehouse, P. L.: Glacial isostatic adjustment modelling: Historical perspectives, recent advances, and future directions, Earth Surface Dynamics, 6, 401–429, https://doi.org/10.5194/esurf-6-401-2018, 2018.

Whitehouse, P. L., Latychev, K., Milne, G. A., Mitrovica, J. X., and Kendall, R.: Impact of 3-D Earth structure on Fennoscandian glacial isostatic adjustment: Implications for space-geodetic estimates of present-day crustal deformations, Geophysical Research Letters, 33, 3–7, https://doi.org/10.1029/2006GL026568, 2006.

Whitehouse, P. L., Gomez, N., King, M. A., and Wiens, D. A.: Solid Earth change and the evolution of the Antarctic Ice Sheet, Nature Communications, 10, 1–14, https://doi.org/10.1038/s41467-018-08068-y, http://dx.doi.org/10.1038/s41467-018-08068-y, 2019.

Willeit, M. and Ganopolski, A.: The importance of snow albedo for ice sheet evolution over the last glacial cycle, Climate of the Past, 14, 697–707, https://doi.org/10.5194/cp-14-697-2018, 2018.

Willeit, M., Ganopolski, A., Calov, R., and Brovkin, V.: Mid-Pleistocene transition in glacial cycles explained by declining CO2 and regolith removal, Science Advances, 5, 1–9, https://doi.org/10.1126/sciadv.aav7337, 2019.

Winkelmann, R., Martin, M. A., Haseloff, M., Albrecht, T., Bueler, E., Khroulev, C., and Levermann, A.: The Potsdam Parallel Ice Sheet Model (PISM-PIK) – Part 1: Model description, The Cryosphere, 5, 715–726, https://doi.org/10.5194/tc-5-715-2011, https://www.the-cryosphere.net/5/715/2011/, 2011.

Zeitz, M., Levermann, A., and Winkelmann, R.: Sensitivity of ice loss to uncertainty in flow law parameters in an idealized one-dimensional geometry, The Cryosphere, 14, 3537–3550, https://doi.org/10.5194/tc-14-3537-2020, https://tc.copernicus.org/articles/14/3537/2020/, 2020.

Zweck, C. and Huybrechts, P.: Modeling of the northern hemisphere ice sheets during the last glacial cycle and glaciological sensitivity, Journal of Geophysical Research Atmospheres, 110, 1–24, https://doi.org/10.1029/2004JD005489, 2005.

Zweng, M. M., Reagan, J. R., Seidov, D., Boyer, T. P., Locarnini, R. A., Garcia, H. E., Mishonov, A. V., Baranova, O. K., Weathers, K. W., Paver, C. R., and Smolyar, I. V.: WORLD OCEAN ATLAS 2018 Volume 2: Salinity, Tech. Rep. September, 2018.